RESEARCH MEMORANDUM

EXPERIMENTAL INVESTIGATION OF THE ZERO-LIFT WAVE DRAG OF SEVEN PAIRS OF DELTA WINGS WITH CONSTANT AND VARYING THICKNESS RATIOS AT MACH NUMBERS OF 1.62, 1.93, AND 2.41

By Arthur Henderson, Jr.

Langley Aeronautical Laboratory
Langley Field, Va.

NATIONAL ADVISORY COMMITTEE
FOR AERONAUTICS

WASHINGTON

June 3, 1955

NATIONAL ADVISORY COMMITTEE FOR AERONAUTICS

RESEARCH MEMORANDUM

EXPERIMENTAL INVESTIGATION OF THE ZERO-LIFT WAVE DRAG OF SEVEN PAIRS OF DELTA WINGS WITH CONSTANT AND VARYING THICKNESS RATIOS AT MACH NUMBERS OF 1.62, 1.93, AND 2.41

By Arthur Henderson, Jr.

SUMMARY

Seven pairs of wings were tested at Mach numbers of 1.62, 1.93, and 2.41 to ascertain the validity of NACA TN 2858, which predicts that a delta wing with optimum linearly varying thickness ratio will have less wave drag than a constant-thickness-ratio delta wing when both wings have the same plan form, ridge-line position, and either the same frontal area or the same volume. It is shown that, except when the assumptions of linear theory are grossly violated, the theoretical and experimental results are in qualitative agreement, with wave-drag reductions of as much as 15 percent being realized experimentally.

INTRODUCTION

In reference 1 it was shown by means of linear theory that a rhombic-sectioned delta wing with linearly varying thickness ratio can have less zero-lift wave drag than a corresponding constant-thickness-ratio delta wing when both wings have the same plan form, ridge-line location, and either the same frontal area or the same volume.

The theoretical results of reference 1 showed that, when both wings have the same frontal area, substantial drag reductions can be realized only when both the ridge line and the leading edge are subsonic; whereas, when both wings have the same volume, drag reductions can be obtained throughout the whole supersonic Mach number range (within the limits of linear theory). In some cases, drag reductions in excess of 20 percent are predicted.

These encouraging theoretical results prompted the present investigation, which is an attempt to ascertain the validity of the theory and to determine whether the thickness distribution for lower drag is a critical function of Mach number, that is, whether a wing which is designed to have good drag characteristics at one Mach number will have good drag characteristics at other Mach numbers.

SYMBOLS

D	drag
L	lift
c_r	root chord
$\bar{c}$	mean aerodynamic chord, $\frac{2}{3} c_r$
M	Mach number
$\bar{m}$	thickness-ratio-distribution parameter (see eqs. (1) and (2) and fig. 3)
q	dynamic pressure
R	Reynolds number
r	ridge-line position measured from trailing edge, percent chord
S	wing area
t_r	maximum root thickness
$t(y)$	maximum local thickness
y	spanwise ordinate
α	angle of attack, deg
$\beta = \sqrt{M^2 - 1}$	
δ	probable error in C_D
ϵ	tangent of leading-edge semiapex angle

τ_r root thickness ratio

$\tau(y)$ local thickness ratio

C_L lift coefficient, $\frac{\text{Lift}}{qS}$

C_{L_α} lift-curve slope, per degree, $\left(\frac{\partial C_L}{\partial \alpha}\right)_{\alpha=0^\circ}$

C_D drag coefficient, $\frac{\text{Drag}}{qS}$

C_m pitching-moment coefficient, $\frac{\text{Pitching moment about } \frac{2}{3} c_r}{qS\bar{c}}$

C_{m_α} pitching-moment-curve slope, per degree, $\left(\frac{\partial C_m}{\partial \alpha}\right)_{\alpha=0^\circ}$

A and B wing pairs are numbered 1 to 7. An "A" or "B" following a number designates variable- or constant-thickness-ratio wing, respectively.

Primed symbols refer to constant-thickness-ratio wing.

APPARATUS AND TESTS

Wind Tunnel

The Langley 9-inch supersonic tunnel is a continuous-operation closed-circuit tunnel in which the pressure, temperature, and humidity of the enclosed air can be regulated. Different test Mach numbers are provided by interchangeable nozzle blocks which form test sections approximately 9 inches square. Eleven fine-mesh turbulence-damping screens are installed in the relatively large-area settling chamber ahead of the supersonic nozzle. The turbulence level of the tunnel is considered low, based on past turbulence-level measurements. (See ref. 2.)

Models

The models were sting supported as shown in figure 1(b). Forces and moments were measured on the external three-component strain-gage balance (see fig. 1(a)).

Seven pairs of wings were tested. Each pair consisted of a constant- and a variable-thickness-ratio delta wing. Both wings of a pair had the same plan form, ridge-line position, and either the same frontal area or the same volume. Three pairs of wings were made so that the constant- and variable-thickness-ratio wings of a pair had the same frontal area; the other four pairs, the same volume. All constant-thickness-ratio wings were 6 percent thick. The thickness distributions on the variable-thickness-ratio wings were governed by the requirements that, on a frontal-area basis,

$$\tau(y) = \frac{\tau_r'}{1 + \frac{2}{3}\bar{m}}\left(1 + \frac{2\bar{m}}{c_r\epsilon}y\right) \tag{1}$$

and, on a volume basis,

$$\tau(y) = \frac{\tau_r'}{1 + \frac{1}{2}\bar{m}}\left(1 + \frac{2\bar{m}}{c_r\epsilon}y\right) \tag{2}$$

The quantity $\bar{m}$ was determined from the charts of reference 1 after certain values of $\beta\epsilon$ and a ridge-line position have been arbitrarily chosen. The wings were then constructed so that the optimum linearly varying thickness ratio was obtained for $M = 1.93$.

The geometric characteristics of the delta wings are given in figure 2 and table I. Photographs of the wings are presented in figure 3.

Test Methods

The tests were run through an angle-of-attack range from -2° to about 6°. Thus, in addition to zero-lift drag, the second-order effects of thickness distribution on lift and pitching moment were also obtained.

It has been shown (ref. 3) that the contribution of the sting to the lift and pitching moment of the test results is negligible. Unpublished data from the Langley 9-inch supersonic tunnel on sting interference on delta wings show by means of pressure measurements that, as far as drag is concerned, the combination of wing and sting is essentially the same as wing alone, for, although the sting is subject to a drag force, its presence superimposes a higher pressure field on a portion of the reverse slope of the wing in such a way that these two effects tend to be compensating. Thus, in the present investigation, no correction for sting effect has been applied.

During the tests it was found that the deflection of the strain-gage-balance beams under load caused the sting to become antisymetrically displaced with respect to the sting shield so that, at the higher angles of attack, one or two side edges of the sting shield were exposed to the free stream, causing a variation of pressure on the sting shoulder. Therefore, pressure measurements were taken on each of the four sting-shield lips. These values were assumed to be the pressures acting on the sting shoulder. A correction was applied to the drag in order to account for the difference between these pressures and free-stream pressure and the difference between the balance-box pressure and the free-stream pressure.

Precision of Data

The estimated probable errors in the aerodynamic quantities are as follows:

M	Probable errors in -					
	C_L	C_D	C_m	M	α, deg	R
1.62	±0.0012	±0.0002	±0.0014	±0.01	±0.05	±20,000
1.93	±.0014	±.0003	±.0014	±.01	±.05	±20,000
2.41	±.0004	±.0001	±.0006	±.01	±.05	±20,000

Reynolds Number

The test Reynolds numbers based on the mean aerodynamic chord are as follows:

Wing	Reynolds number at -		
	M = 1.62	M = 1.93	M = 2.41
1A,1B	4.32×10^6	4.51×10^6	3.92×10^6
2A,2B	4.45	4.70	4.04
3A,3B	4.09	4.29	3.72
4A,4B	4.09	4.29	3.72
5A,5B	4.09	4.29	3.72
6A,6B	4.45	4.70	4.04
7A,7B	2.61	2.74	2.36

RESULTS AND DISCUSSION

Although the primary interest of the investigation is zero-lift wave drag, the values of lift, total drag, pitching moment, and lift-drag ratios for an angle-of-attack range from approximately -2° to 6° are presented in figures 4, 5, and 6 for Mach numbers of 1.62, 1.93, and 2.41, respectively. (Flagged symbols on these figures represent check points.) Figures 7, 8, and 9 present, respectively, the variation with Mach number of C_{L_α}, C_{m_α}, and location of the aerodynamic center in percent of the mean aerodynamic chord.

An examination of figures 7, 8, and 9 shows that, except for wings 7, the second-order effects of thickness distribution on C_{L_α}, C_{m_α}, and location of the aerodynamic center are negligible. The reason that C_{L_α} for wing 7A is lower than C_{L_α} for wing 7B is indirectly associated with thickness distribution. The thickness distribution of wing 7A, which has a relatively large span, is such that the wing tips are flexible. The associated aeroelastic effects create a loss in lift at the tips.

Figures 4 to 6 show that the ratios of L/D follow the trends which would be expected; that is, the wing with the lower minimum drag generally has a higher ratio of L/D.

Figure 10 presents the ratio of the zero-lift drag of the variable-thickness-ratio wing to the zero-lift drag of the constant-thickness-ratio wing. It should be noted that these drag ratios, which are obtained from measured quantities, are subject to error. Each point on figure 10, therefore, represents the mean of a short vertical band of possible points, the extremes of which are $\frac{C_D + \delta}{C_D' - \delta}$ and $\frac{C_D - \delta}{C_D' + \delta}$, where δ is the probable error in drag coefficient. It should be understood then that the variable-thickness-ratio wings which are shown to have small drag reductions may possibly have little or no drag reduction, or, of course, they could have more than is shown. Thus, the drag ratio of wings 1 (flagged symbol) which is shown to be about 0.93 at $M = 1.62$ could possibly be a maximum of 0.98 or a minimum of 0.87. The unflagged symbols represent the total-drag ratios, whereas the flagged symbols are for the drag ratios with an assumed skin-friction drag removed (that is, they are taken to be the wave-drag ratios). The solid lines represent the theory of reference 1. The skin-friction drag was calculated by assuming laminar flow (Blasius theory) ahead of the ridge line and turbulent flow (Frankl-Voishel extended theory) behind the ridge line. This is known to be a fairly good assumption for constant-thickness-ratio wings. For variable-thickness-ratio wings the validity of this assumption is not so clear, for behind those sections of the ridge line

where the thickness ratio is less than that of the constant-thickness-ratio wing, the disturbances which tend to trip transition would be less. In order to check the validity of applying the same boundary-layer assumption to both wings, a liquid-film study was made of wings 4A and 4B at $M = 2.41$ and $R = 3.72 \times 10^6$. These wings were chosen because they had the lowest drag ratio. It may be seen from figure 11 that both wings had essentially the same boundary-layer pattern. Thus, although the particular assumption made as to the extent of laminar and turbulent flow may not be correct, assuming that both wings have the same boundary-layer distribution appears to be quite acceptable. Since the true friction drag is probably somewhat less than that calculated (with a smaller turbulent region than assumed), the true wave-drag ratio lies between the flagged and unflagged symbols of figure 10.

Wing pairs 1 to 3 were constructed on a frontal-area basis, whereas pairs 4 to 7 were made on a volume basis. Figure 10 shows that one wing of each of these sets (3A and 6A) did not come up to expectations (that is, the experimental drag ratios of wings 3A and 3B and wings 6A and 6B were greater than 1). Of the remaining wings it may be seen that, at the design Mach number ($M = 1.93$), the variable-thickness-ratio wings with the same volume as their corresponding constant-thickness-ratio wings had relatively better experimental drag characteristics than the variable-thickness-ratio wings of the frontal-area series. This is in line with the results of reference 1. It should be noted that wings 1A, 3A, and 6A had positive values of $\bar{m}$ (maximum thickness ratio at the tip), and all of the drag ratios were above values calculated by theory. Of these wings, only wing 1A gave a drag reduction, which was about 7 percent as compared to the theoretical value of 13 percent at $M = 1.93$ (design Mach number). The other four variable-thickness-ratio wings had negative values of $\bar{m}$ (maximum thickness ratio at the root) and their experimental results were all in qualitative agreement with theory.

The ridge-line positions on the three wings with positive $\bar{m}$ thickness distributions, were well forward which, as may be seen from table II, caused the outboard sections of the forward slopes to have fairly high flow-deflection angles.

By considering the worst case, that of wing pair 6, the forward slope of wing 6B is seen to have a flow-deflection angle of 16.7°; this clearly violates the assumption of small disturbances. Since 67 percent of the frontal area of wing 6A has flow-deflection angles in excess of 16.7°, it would be expected that the discrepancy between theory and experiment would be greater for wings 6A than for wings 6B. This is borne out by figure 10. These slopes can be reduced by either moving the ridge line rearward or reducing the thickness ratio of the constant-thickness-ratio wing by some factor which will reduce all the slopes of the variable-thickness-ratio wing by the same factor. Both of these methods will make the forward slopes more compatible with linear theory.

But reference 1 shows that, even if the small-disturbance condition is satisfied, moving the ridge line rearward will give very little drag reduction for positive $\bar{m}$ thickness distributions. If the ridge line is allowed to remain where it is and the thickness ratios are reduced to the point where the small-disturbance assumption of linear theory is met, the wave drag of the resulting wing would be such a small portion of the total drag that even a substantial reduction of the wave drag of the variable-thickness-ratio wing over that of the constant-thickness-ratio wing would result in very little total-drag benefit. From the experimental results of this paper and the foregoing considerations, it would therefore appear that the positive $\bar{m}$ thickness distributions of reference 1 are generally of little practical interest.

For the wings with a negative $\bar{m}$ thickness distribution, table II shows that nowhere do the flow-deflection angles of the variable-thickness-ratio wings greatly exceed the values of the corresponding constant-thickness-ratio wing, so that, even if the small disturbance assumption is violated on the B wings, it is not violated much more on the A wings. Therefore, the theoretical predictions for both the B and A wings should have about the same degree of accuracy. The drag-ratio predictions then, although not to be taken quantitatively, should be qualitatively correct, as shown on figure 10.

Figure 10 also shows that the variable-thickness-ratio wings which gave drag reductions at the design Mach number also gave drag reductions at $M = 1.62$ and $M = 2.41$, although at these Mach numbers the linearly varying thickness ratio was no longer optimum. Thus, within the scope of these tests, it may be concluded that, in general, the thickness distribution for drag reduction is not a critical function of Mach number.

CONCLUDING REMARKS

In order to check the validity of the zero-lift wave-drag predictions of NACA TN 2858, seven pairs of wings have been tested at Mach numbers of 1.62, 1.93, and 2.41. Each pair consisted of a variable- and a constant-thickness-ratio wing; both wings of a pair had the same plan form, ridge-line position, and either the same frontal area or the same volume. For either of these conditions, the criteria of NACA TN 2858 were met for a Mach number of 1.93. Within the scope of these tests, the following conclusions have been drawn:

1. Varying the thickness ratio of a delta wing according to the results of NACA TN 2858 so that the wing has the same volume as a corresponding constant-thickness-ratio wing results in greater drag benefits than are obtained by varying the thickness ratio to give the wing the same frontal area. This bears out the results of NACA TN 2858.

2. There are two types of linearly varying thickness-ratio distribution. The first has the maximum thickness ratio at the root and decreases linearly toward the tip; the second has the minimum thickness ratio at the root and increases linearly toward the tip. Of these two types, the second (minimum thickness ratio at the root) is of little practical interest. Results for wings with the first type of thickness-ratio distribution were consistently in qualitative agreement with theory.

3. The thickness distribution for drag reduction is not a critical function of Mach number. Wings which gave drag reductions at the design Mach number of 1.93 also gave drag reductions at Mach numbers of 1.62 and 2.41.

Langley Aeronautical Laboratory,
National Advisory Committee for Aeronautics,
Langley Field, Va., March 24, 1955.

REFERENCES

1. Henderson, Arthur, Jr.: Supersonic Wave Drag of Nonlifting Delta Wings With Linearly Varying Thickness Ratio. NACA TN 2858, 1952.

2. Love, Eugene S., Coletti, Donald E., and Bromm, August F., Jr.: Investigation of the Variation With Reynolds Number of the Base, Wave, and Skin-Friction Drag of a Parabolic Body of Revolution (NACA RM-10) at Mach Numbers of 1.62, 1.93, and 2.41 in the Langley 9-Inch Supersonic Tunnel. NACA RM L52H21, 1952.

3. Love, Eugene S.: Investigations at Supersonic Speeds of 22 Triangular Wings Representing Two Airfoil Sections for Each of 11 Apex Angles. NACA RM L9D07, 1949.

TABLE I

GEOMETRIC CHARACTERISTICS OF DELTA WINGS TESTED

Wing	$\bar{m}$	$\tan^{-1}\epsilon$	c_r	r	S, sq in.
1A	1.00	20°15'	5.72	0.80	12.04
1B	0	19°56'	5.78	.80	12.11
2A	-.26	16°59'	6.00	.45	10.97
2B	0	16°57'	5.99	.45	10.94
3A	.94	23°12'	5.44	.80	12.69
3B	0	23° 8'	5.48	.80	12.83
4A	-.45	22°39'	5.47	.75	12.50
4B	0	23° 6'	5.48	.75	12.81
5A	-.45	22°57'	5.47	.60	12.66
5B	0	23° 8'	5.48	.60	12.82
6A	.86	16°51'	5.98	.90	10.85
6B	0	17° 0'	5.99	.90	10.96
7A	-.44	42°15'	3.50	.50	11.13
7B	0	42°18'	3.50	.50	11.14

TABLE II

FORWARD AND REAR FLOW-DEFLECTION ANGLES FOR WINGS TESTED

Wing	$y/c_r\epsilon$	Forward slope angle, deg	Rear slope angle, deg
1A ($\bar{m}$ = 1.00)	0	5.1	1.3
	.2	7.2	1.8
	.4	9.2	2.3
	.6	11.2	2.8
	.8	13.2	3.3
	1.0	14.9	4.0
1B	---	8.5	2.1
2A ($\bar{m}$ = -0.264)	0	3.8	4.6
	.2	3.4	4.1
	.4	3.0	3.7
	.6	2.6	3.2
	.8	2.2	2.7
	1.0	1.8	2.2
2B	---	3.1	3.8
3A ($\bar{m}$ = 0.942)	0	5.3	1.3
	.2	7.2	1.8
	.4	9.2	2.3
	.6	11.1	2.8
	.8	13.0	3.3
	1.0	14.9	3.8
3B	---	8.5	2.1
4A ($\bar{m}$ = -0.45)	0	8.8	3.0
	.2	7.2	2.4
	.4	5.7	1.9
	.6	4.1	1.4
	.8	2.5	.8
	1.0	.9	.3
4B	---	6.8	2.3
5A ($\bar{m}$ = -0.45)	0	5.5	3.7
	.2	4.5	3.0
	.4	3.5	2.4
	.6	2.5	1.7
	.8	1.0	1.0
	1.0	.6	.4
5B	---	4.3	2.9
6A ($\bar{m}$ = 0.86)	0	11.9	1.3
	.2	15.7	1.8
	.4	19.5	2.3
	.6	23.1	2.7
	.8	26.5	3.2
	1.0	29.7	3.6
6B	---	16.7	1.9
7A ($\bar{m}$ = -0.44)	0	4.4	4.4
	.2	3.6	3.6
	.4	2.8	2.8
	.6	2.1	2.1
	.8	1.3	1.3
	1.0	.6	.6
7B	---	3.4	3.4

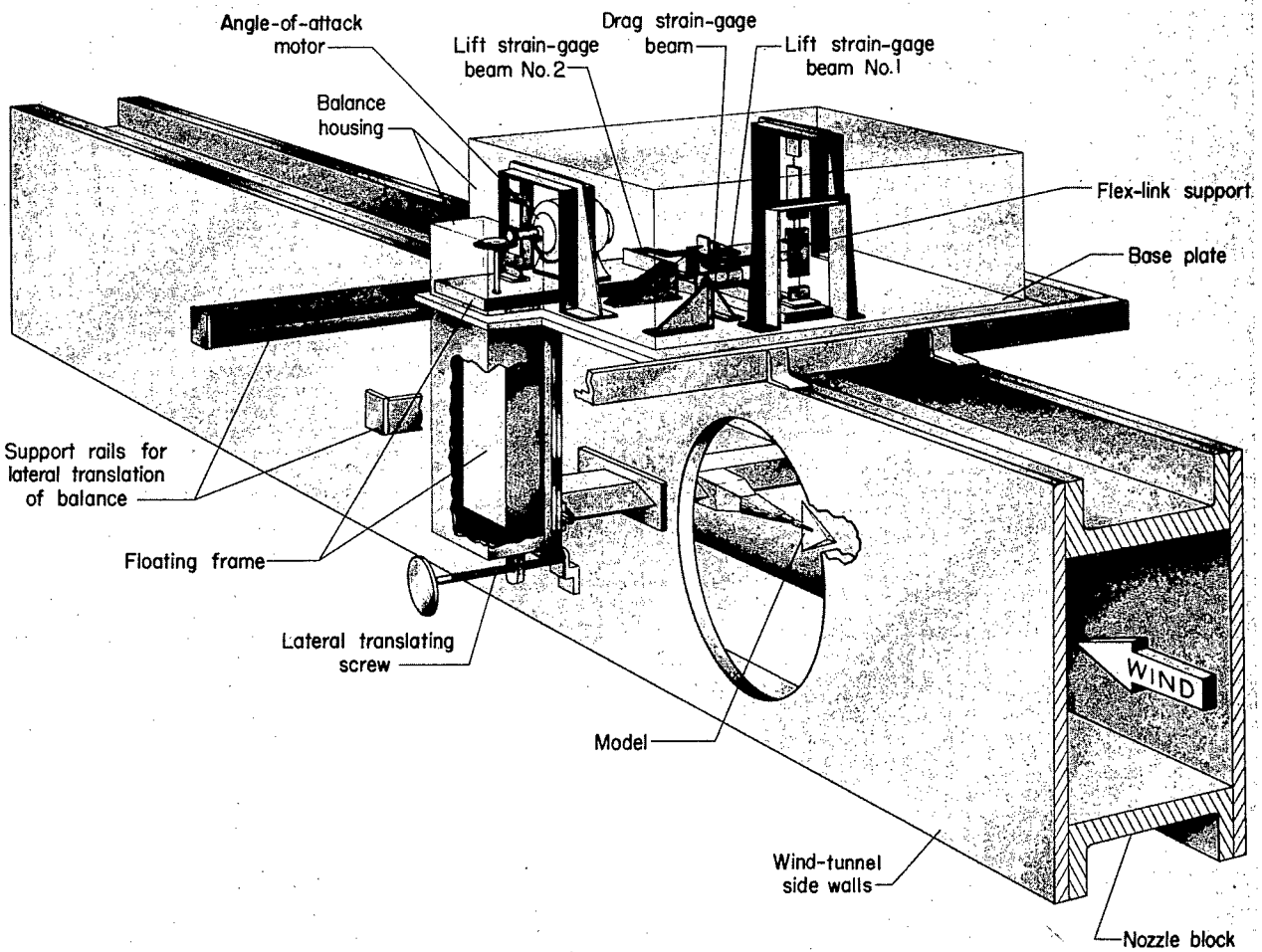

L-87926

(a) Balance.

Figure 1.- Strain-gage balance and model support system.

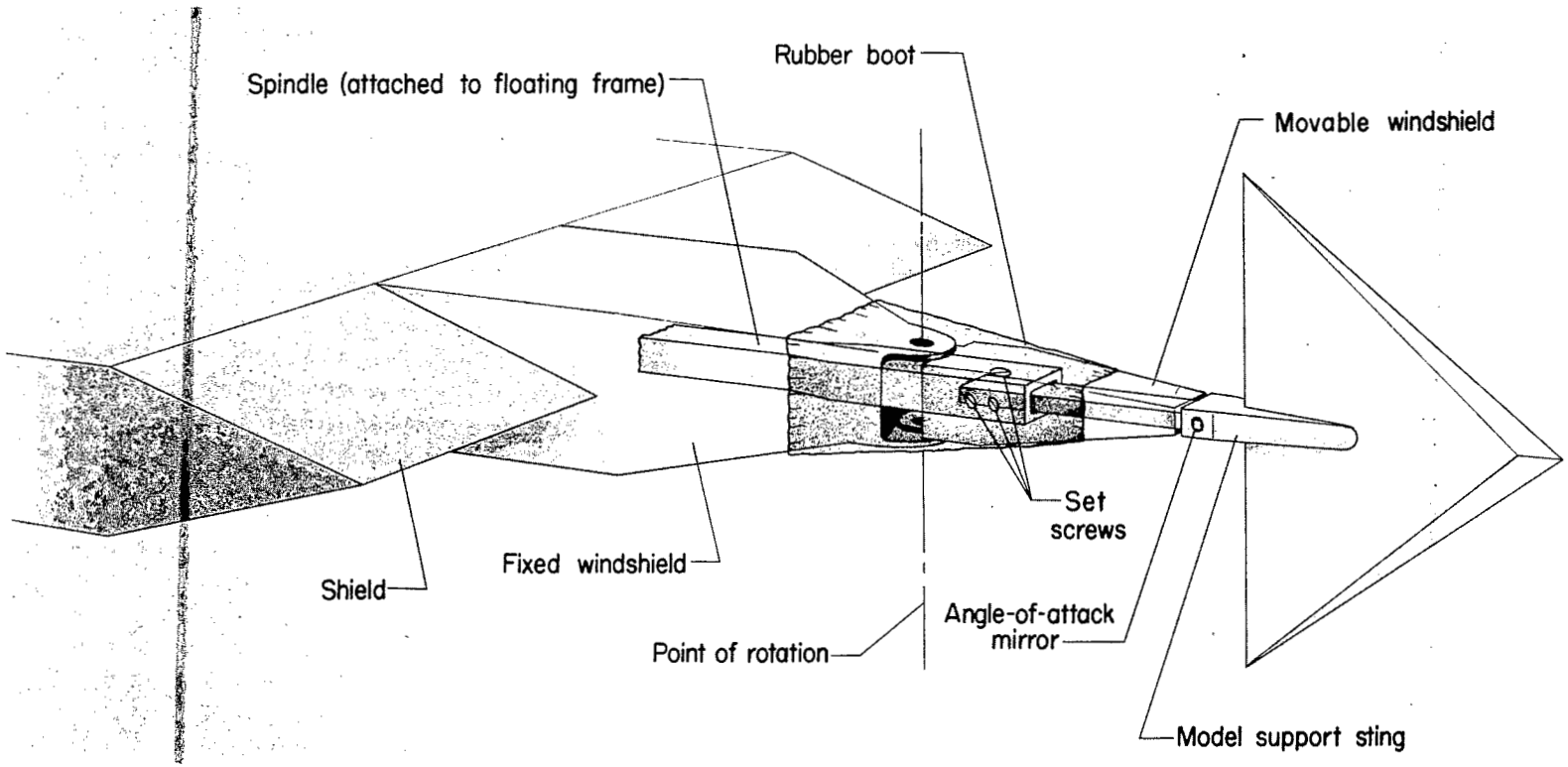

L-87927

(b) Model support system.

Figure 1.- Concluded.

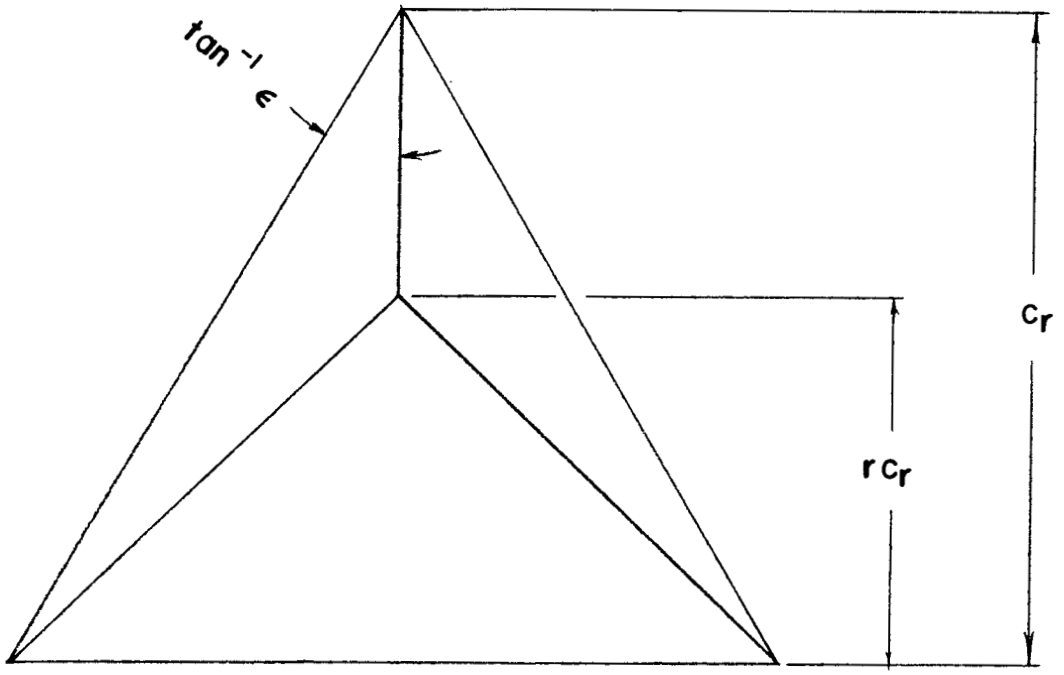

Figure 2.- Pertinent geometric characteristics of delta wings.

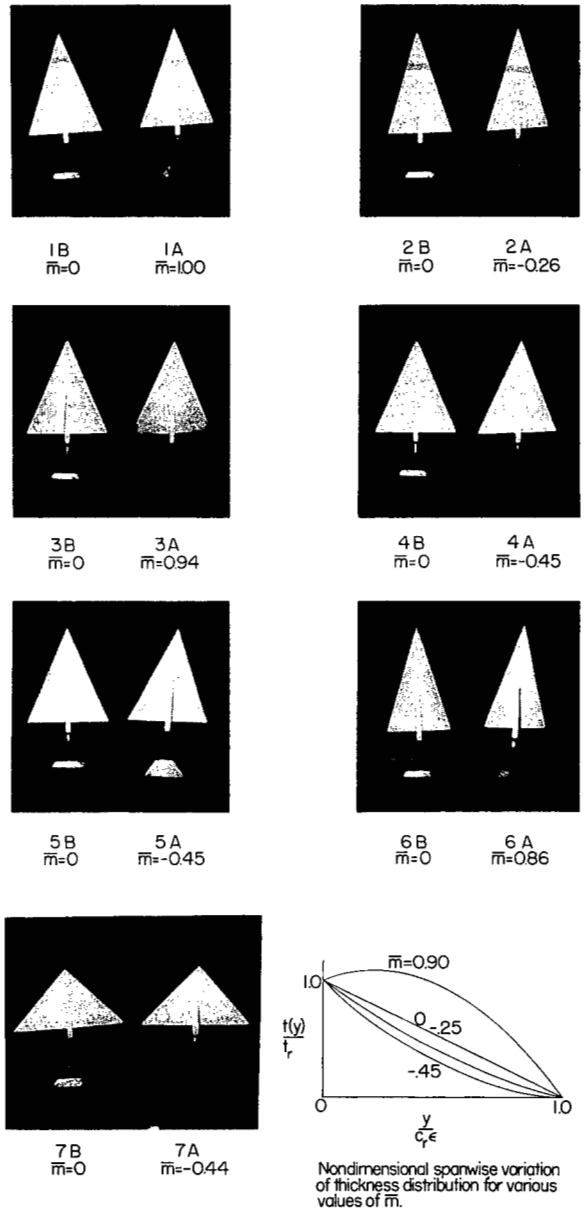

L-87924

Figure 3.- Photographs of the seven pairs of wings used and a sketch of the nondimensional spanwise variation of thickness distribution for various values of $\bar{m}$.

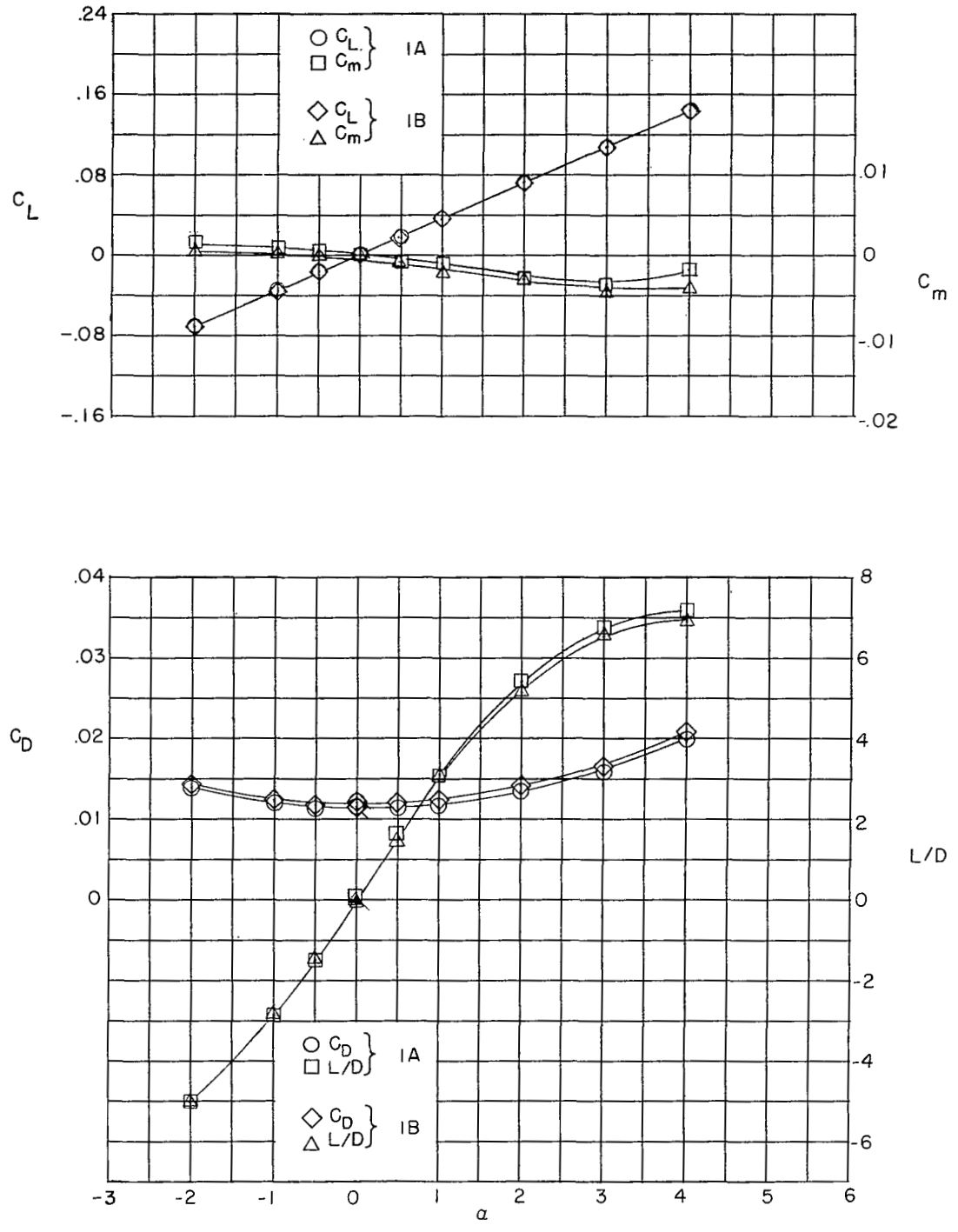

(a) Wings 1A and 1B.

Figure 4.- Aerodynamic characteristics of variable- and constant-thickness-ratio delta wings at M = 1.62. (Flagged symbols represent check points.)

[redacted]

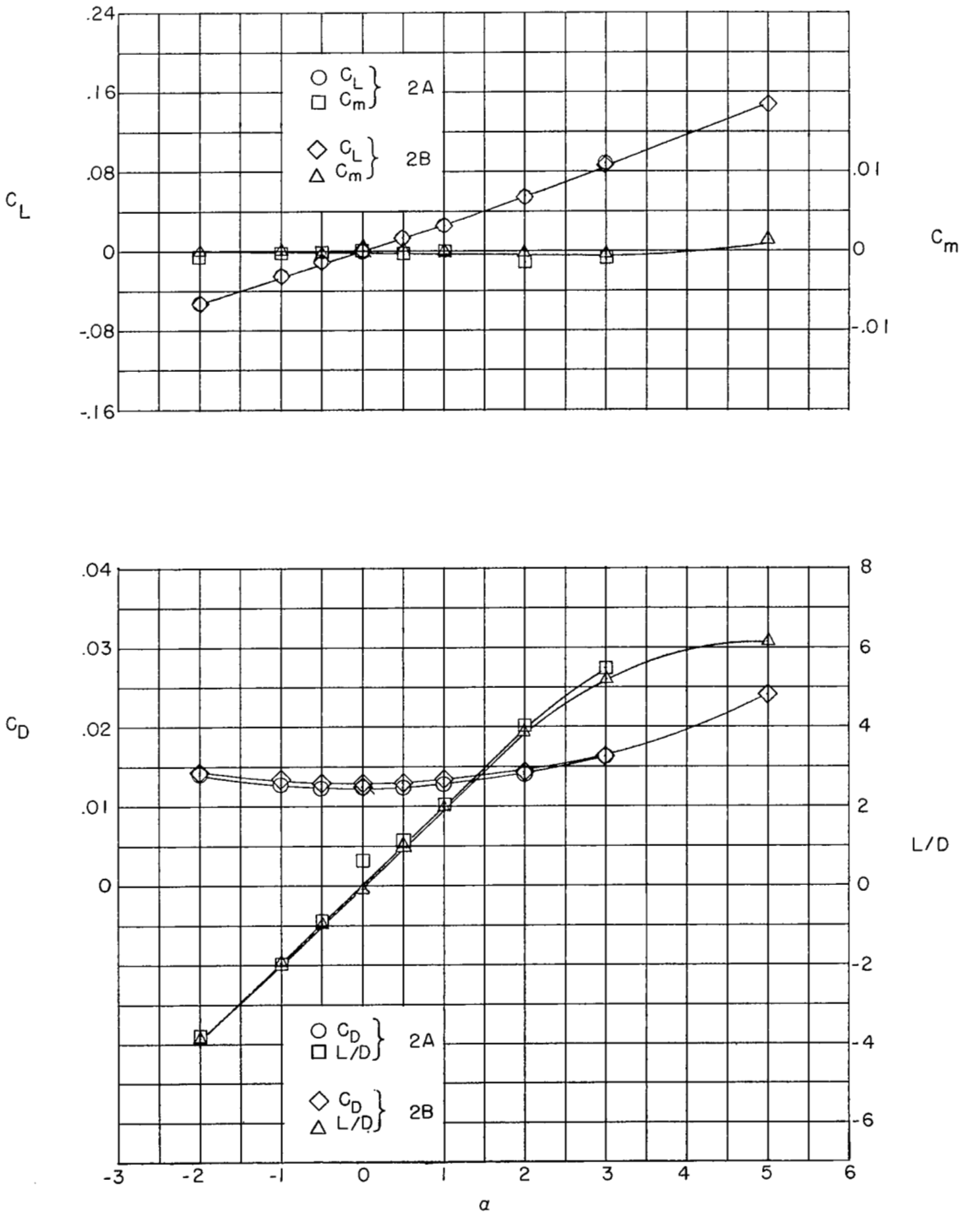

(b) Wings 2A and 2B.

Figure 4.- Continued.

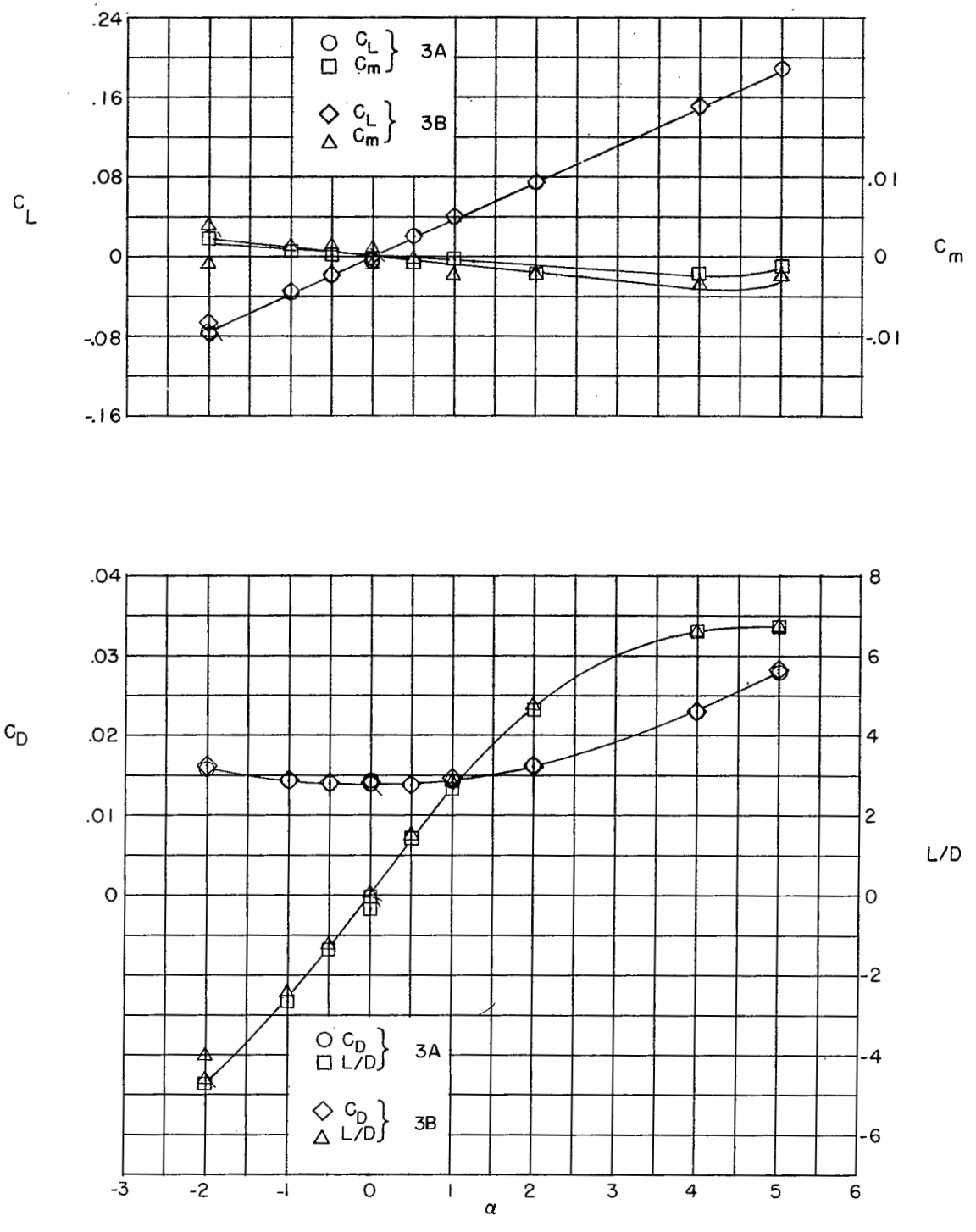

(c) Wings 3A and 3B.

Figure 4.- Continued.

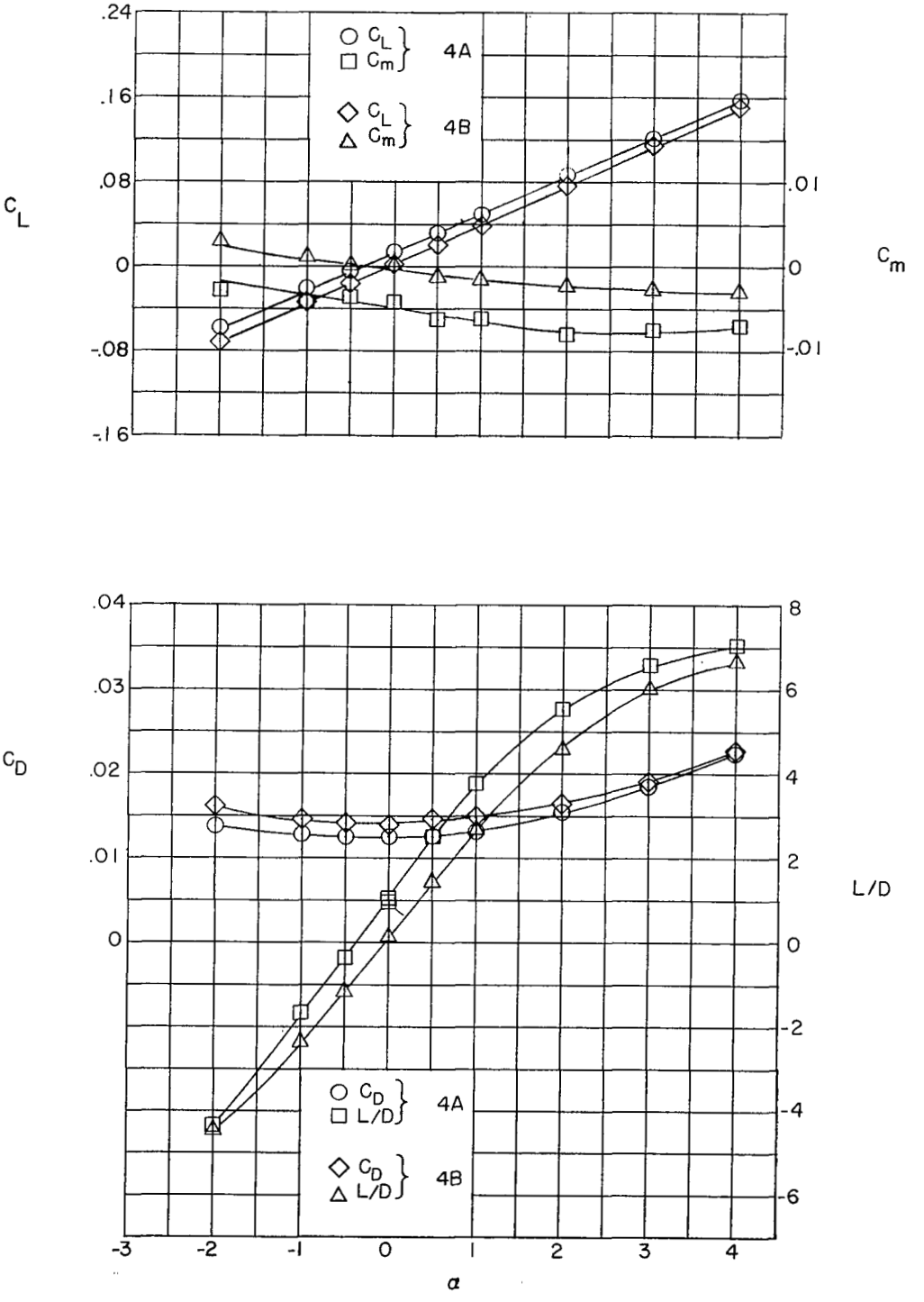

(d) Wings 4A and 4B.

Figure 4.- Continued.

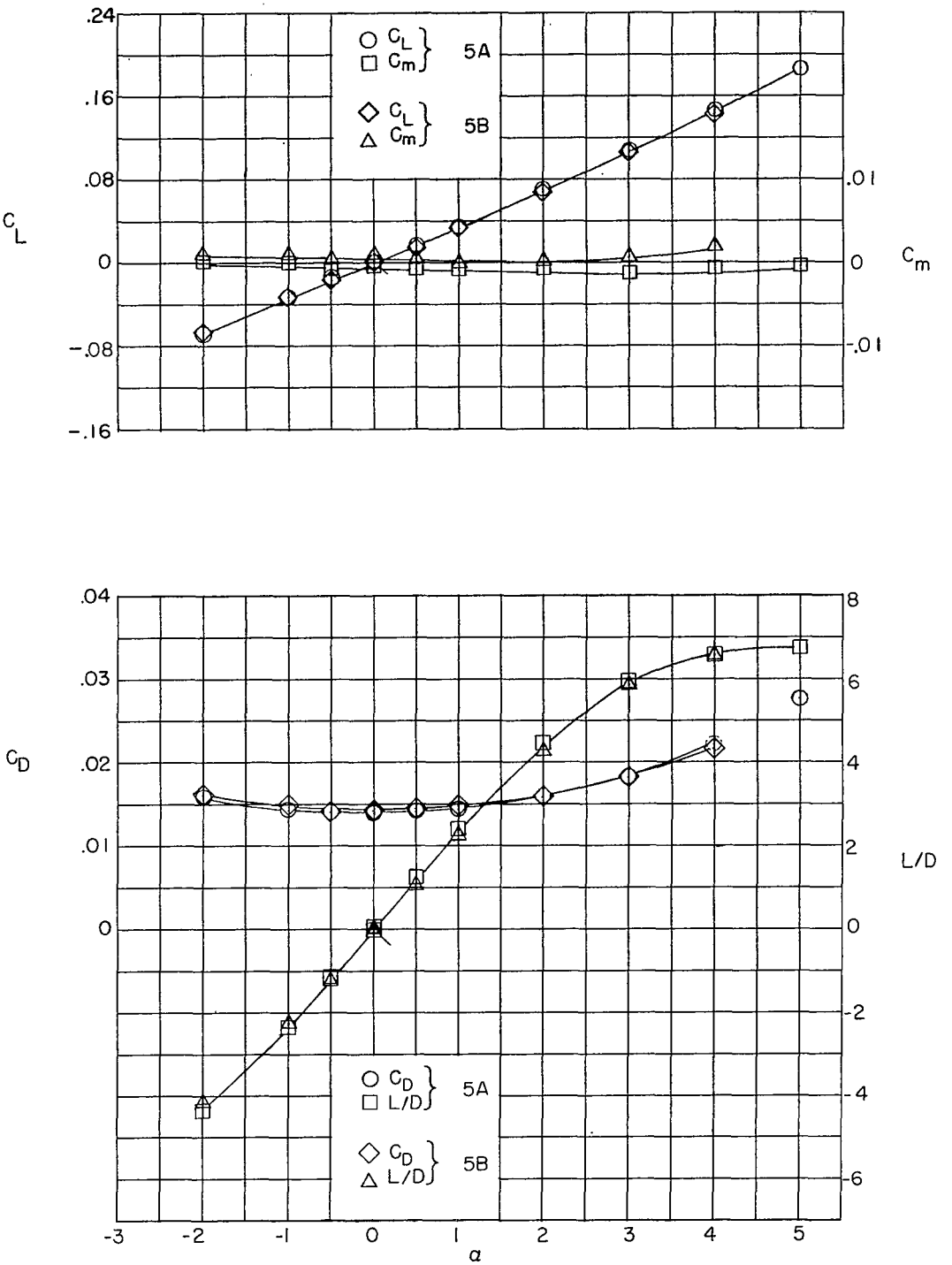

(e) Wings 5A and 5B.

Figure 4.- Continued.

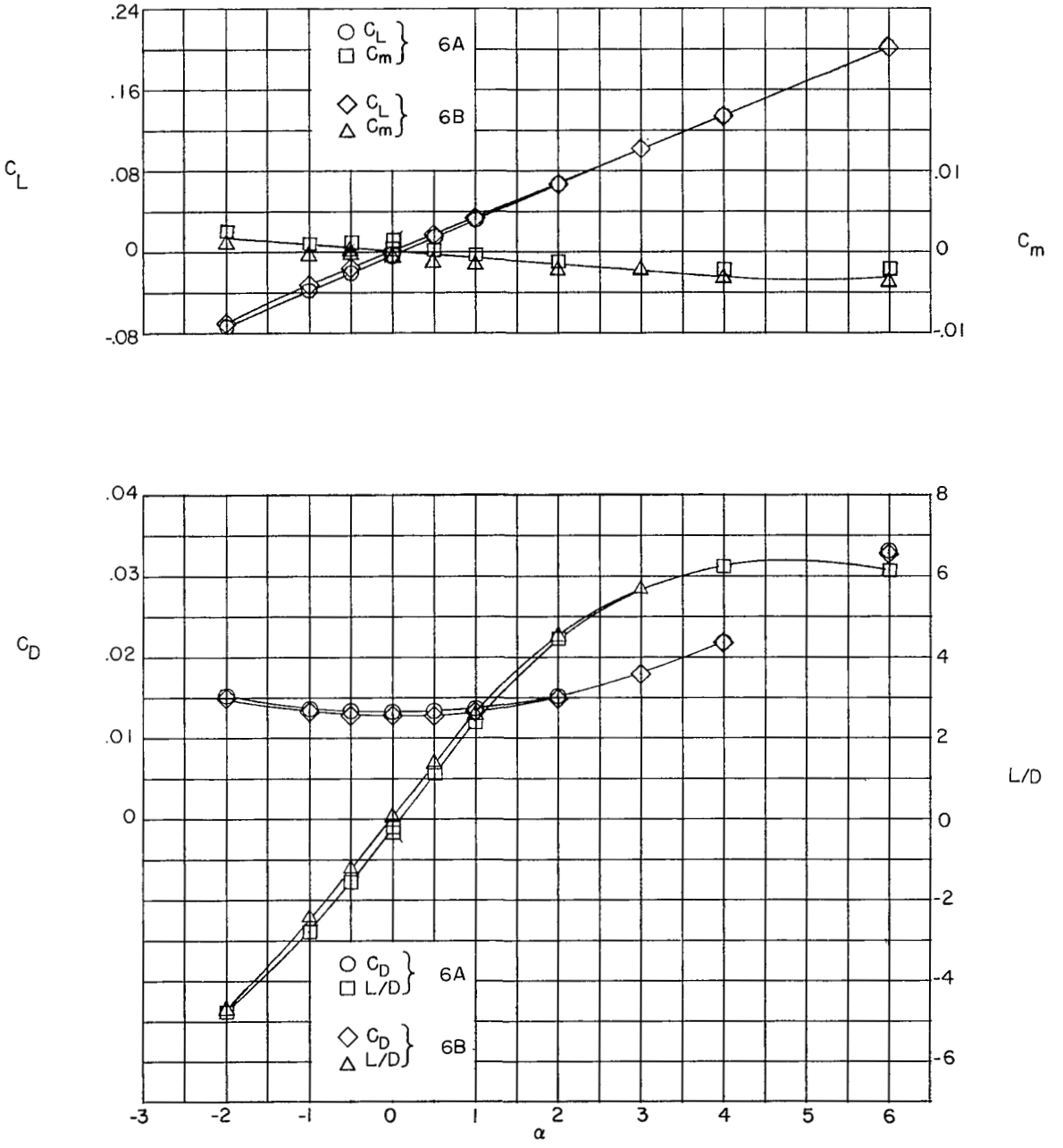

(f) Wings 6A and 6B.

Figure 4.- Continued.

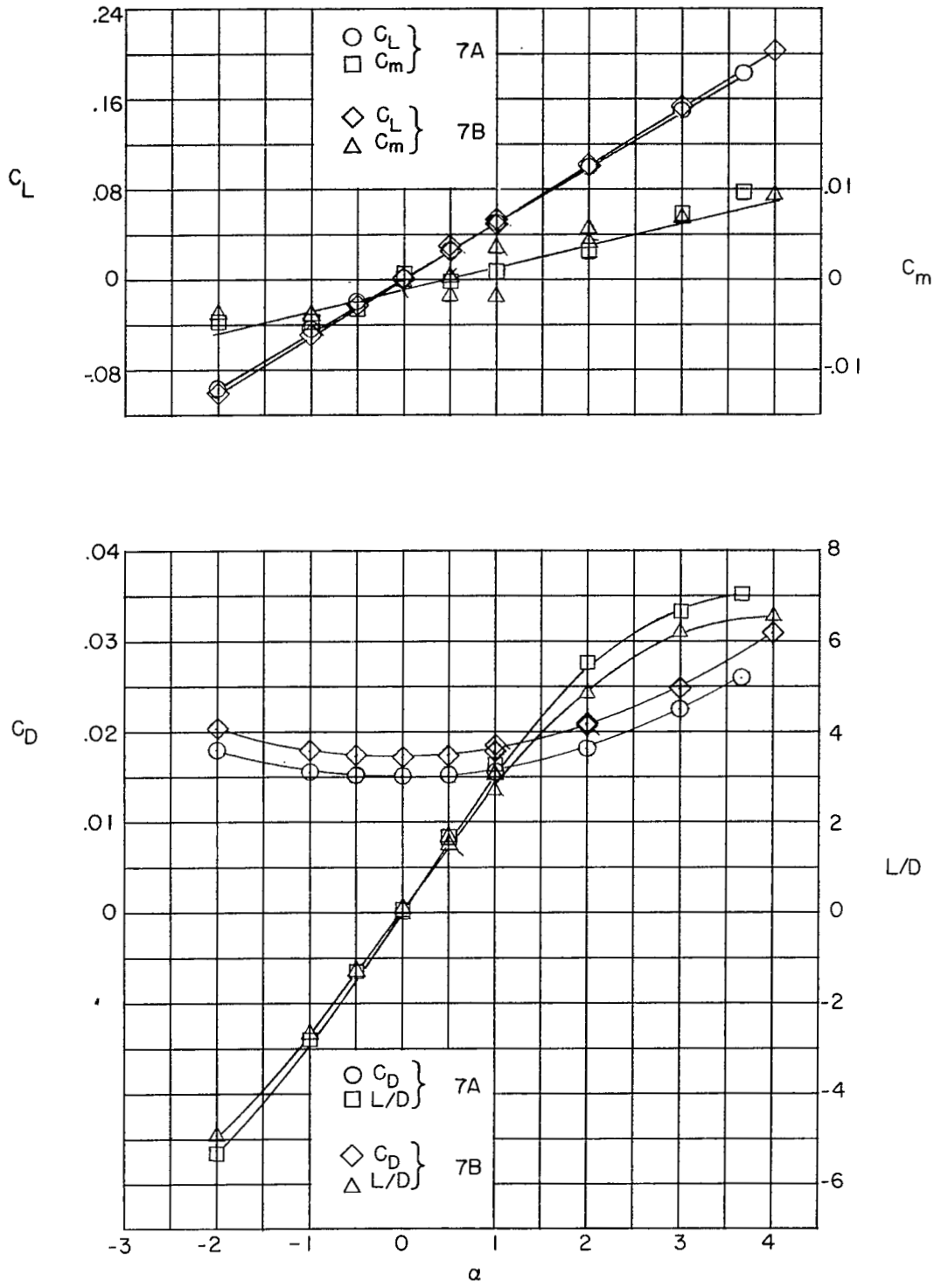

(g) Wings 7A and 7B.

Figure 4.- Concluded.

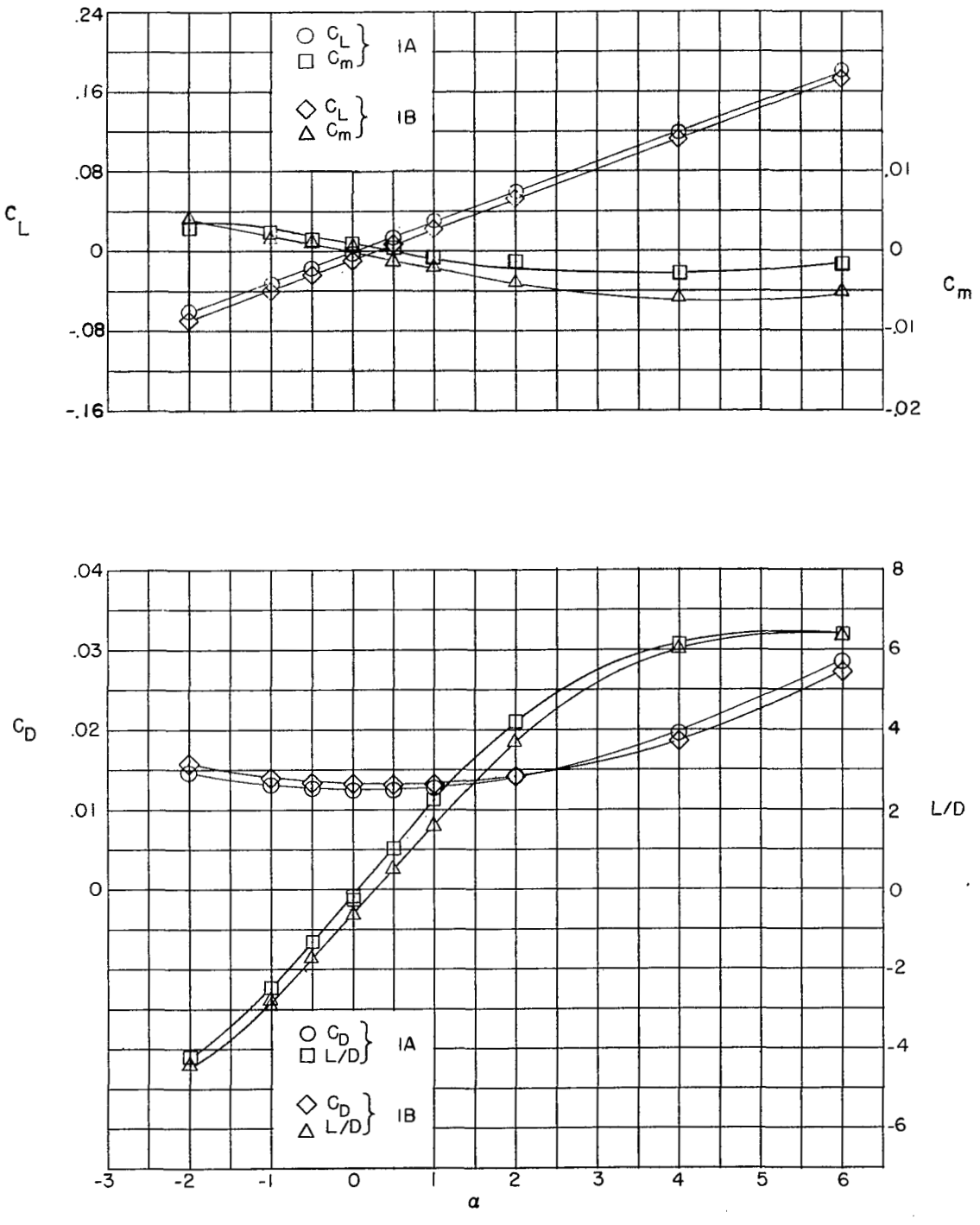

(a) Wings 1A and 1B.

Figure 5.- Aerodynamic characteristics of variable- and constant-thickness-ratio delta wings at M = 1.93. (Flagged symbols represent check points.)

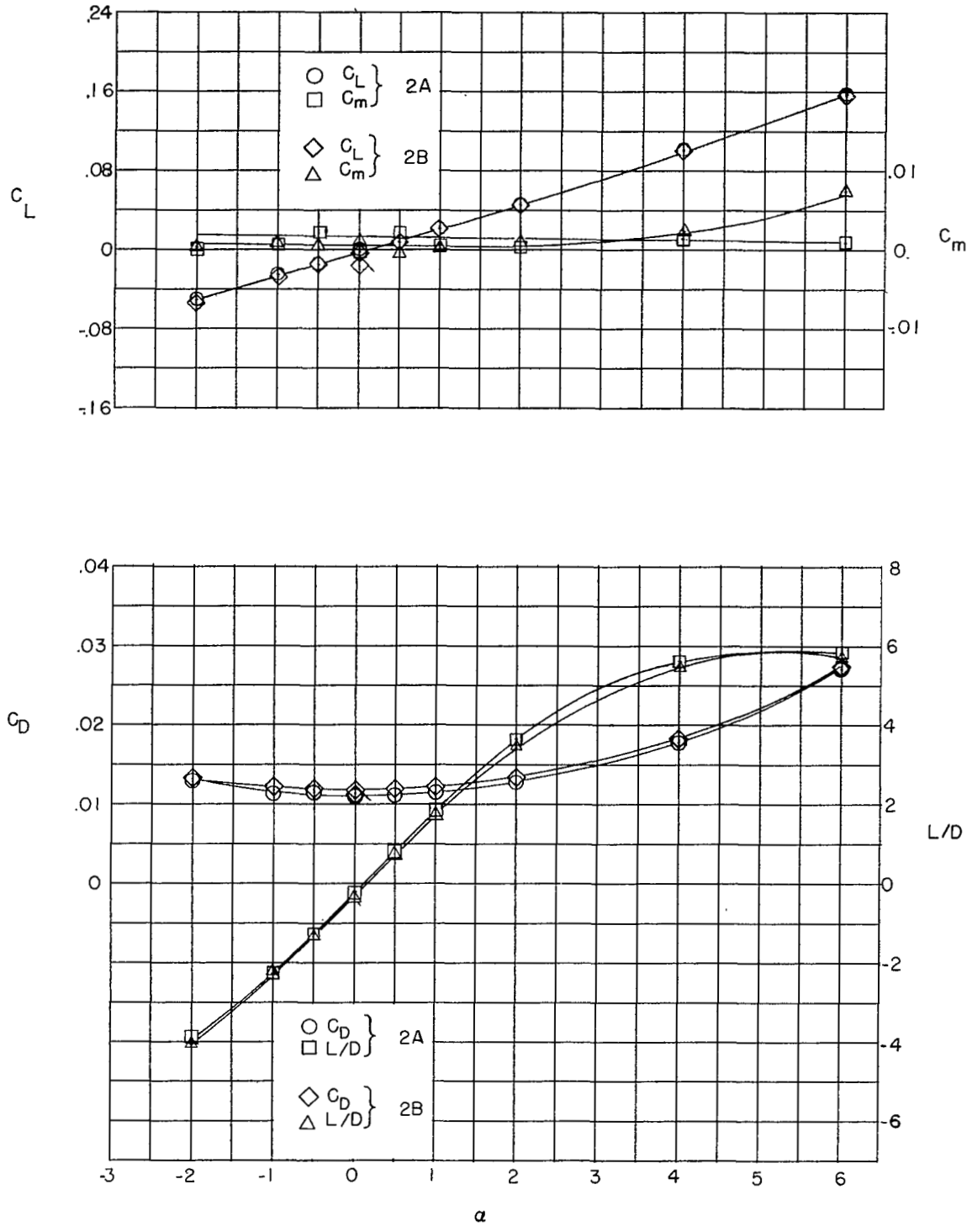

(b) Wings 2A and 2B.

Figure 5.- Continued.

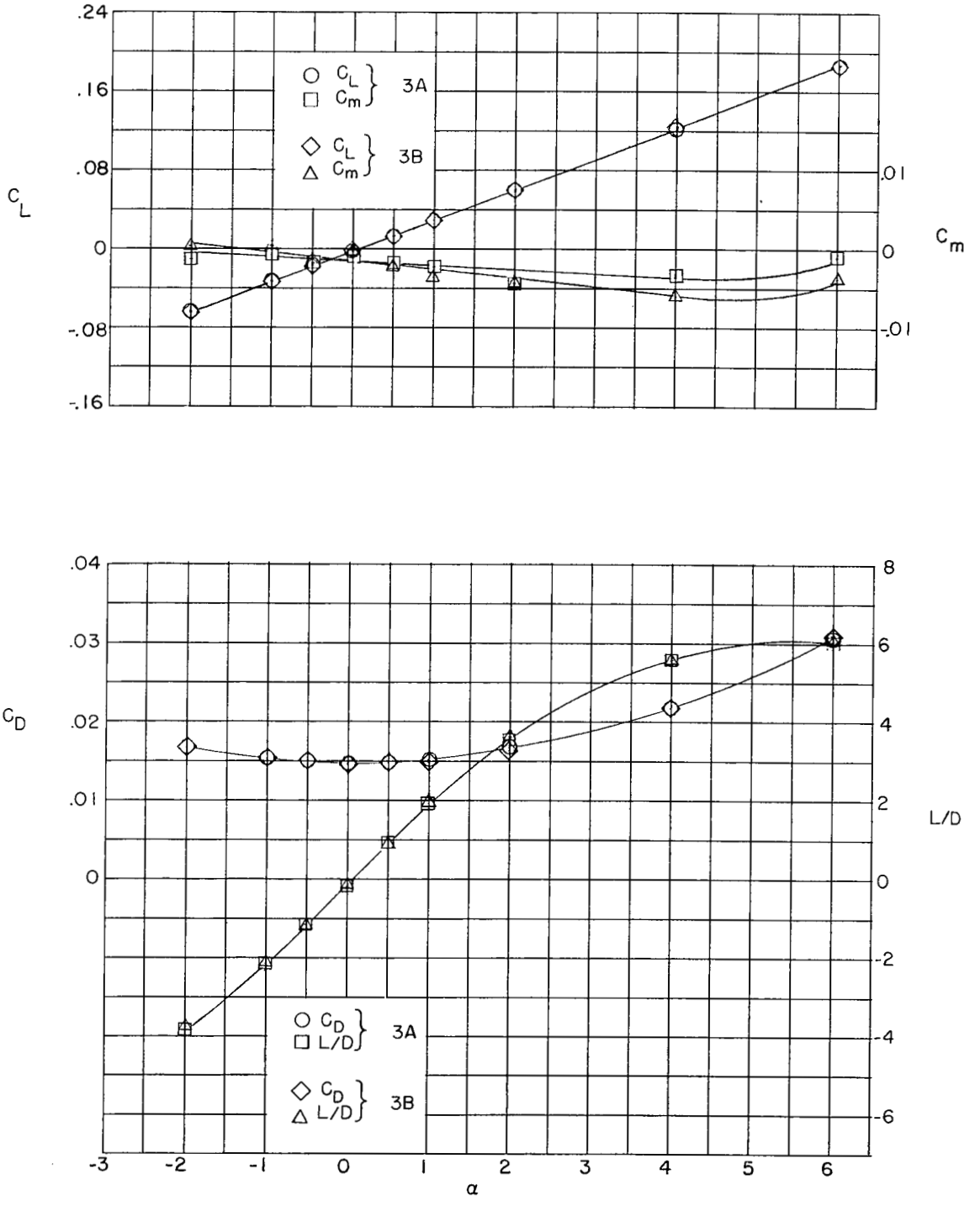

(c) Wings 3A and 3B.

Figure 5.- Continued.

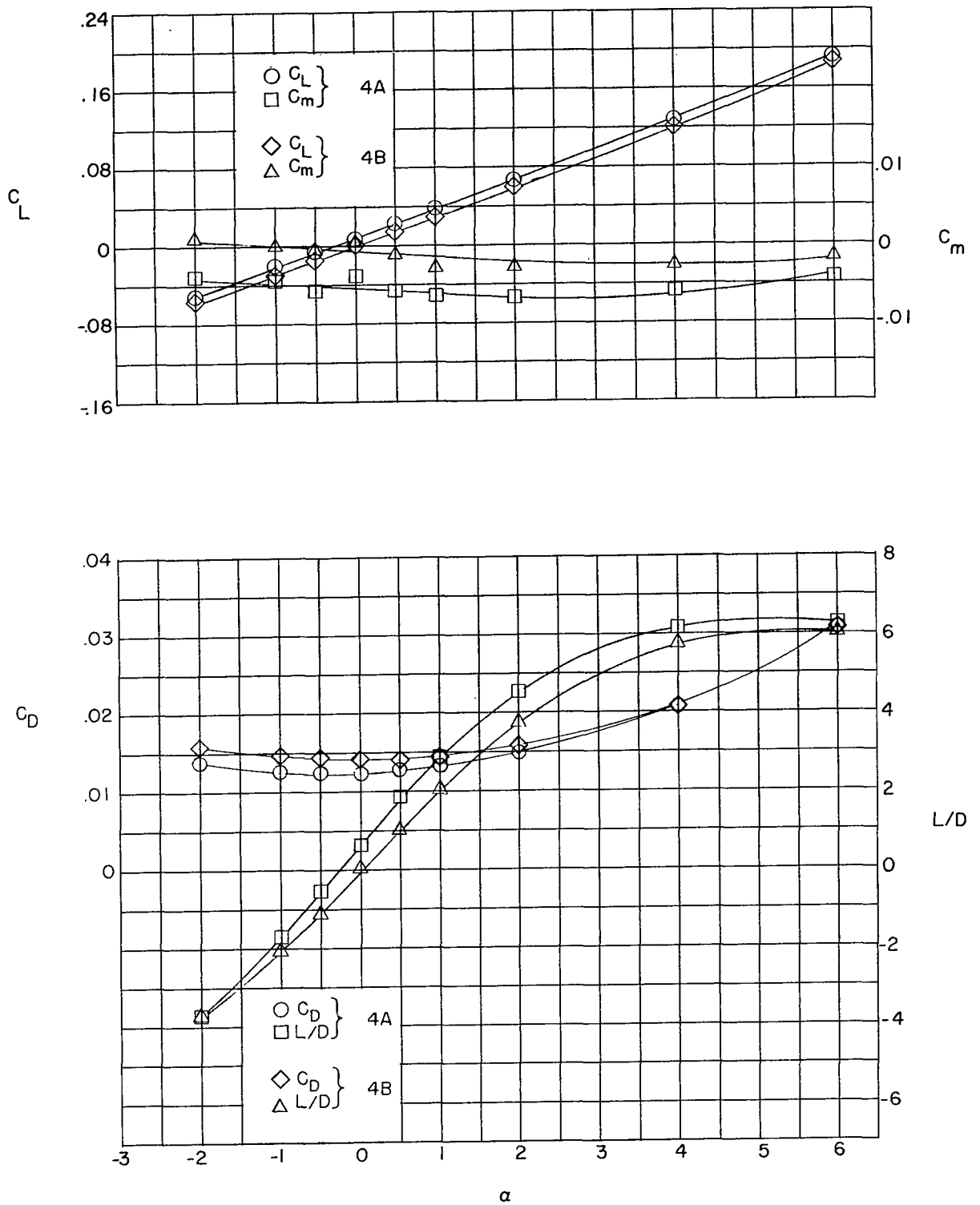

(d) Wings 4A and 4B.

Figure 5.- Continued.

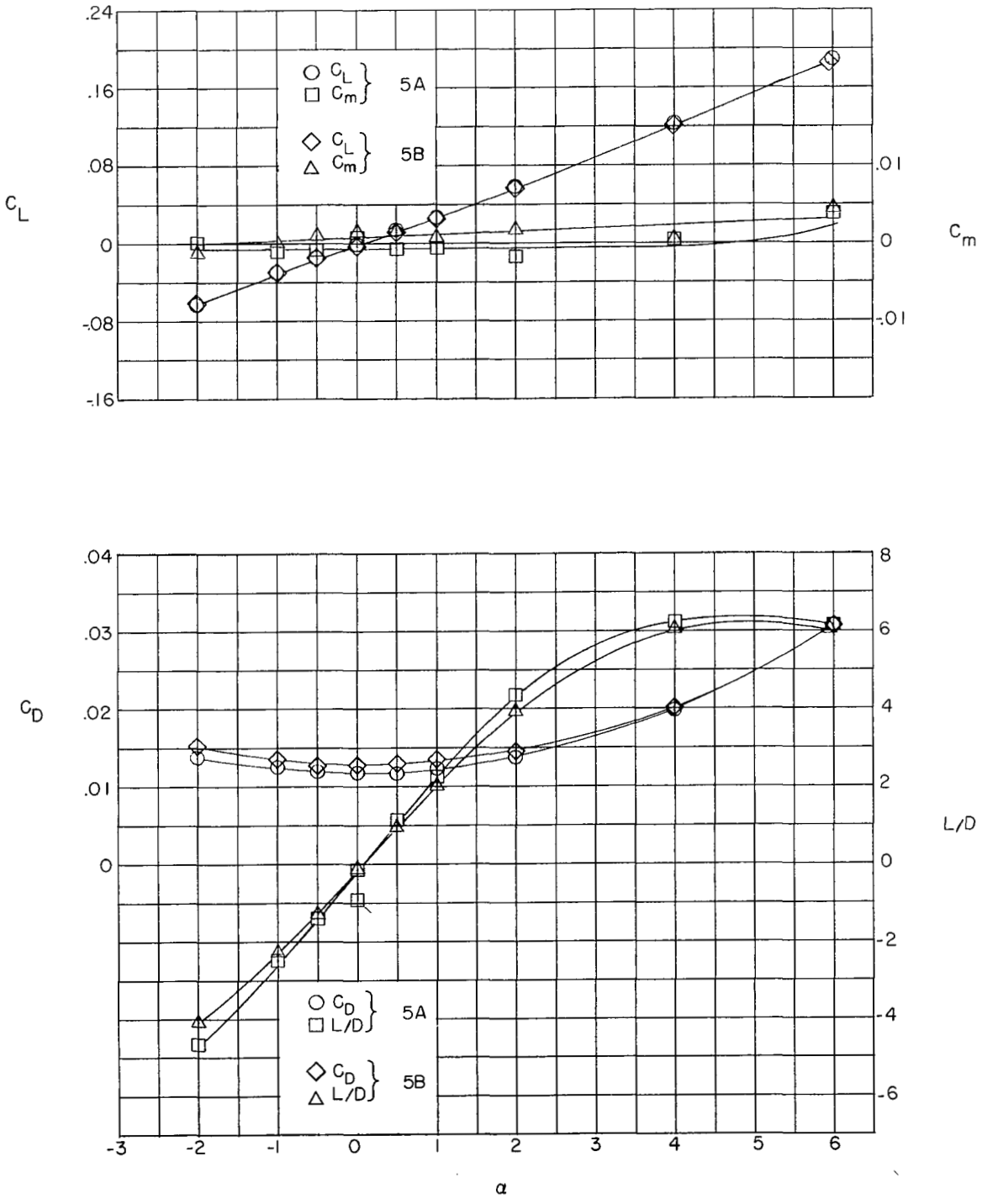

(e) Wings 5A and 5B.

Figure 5.- Continued.

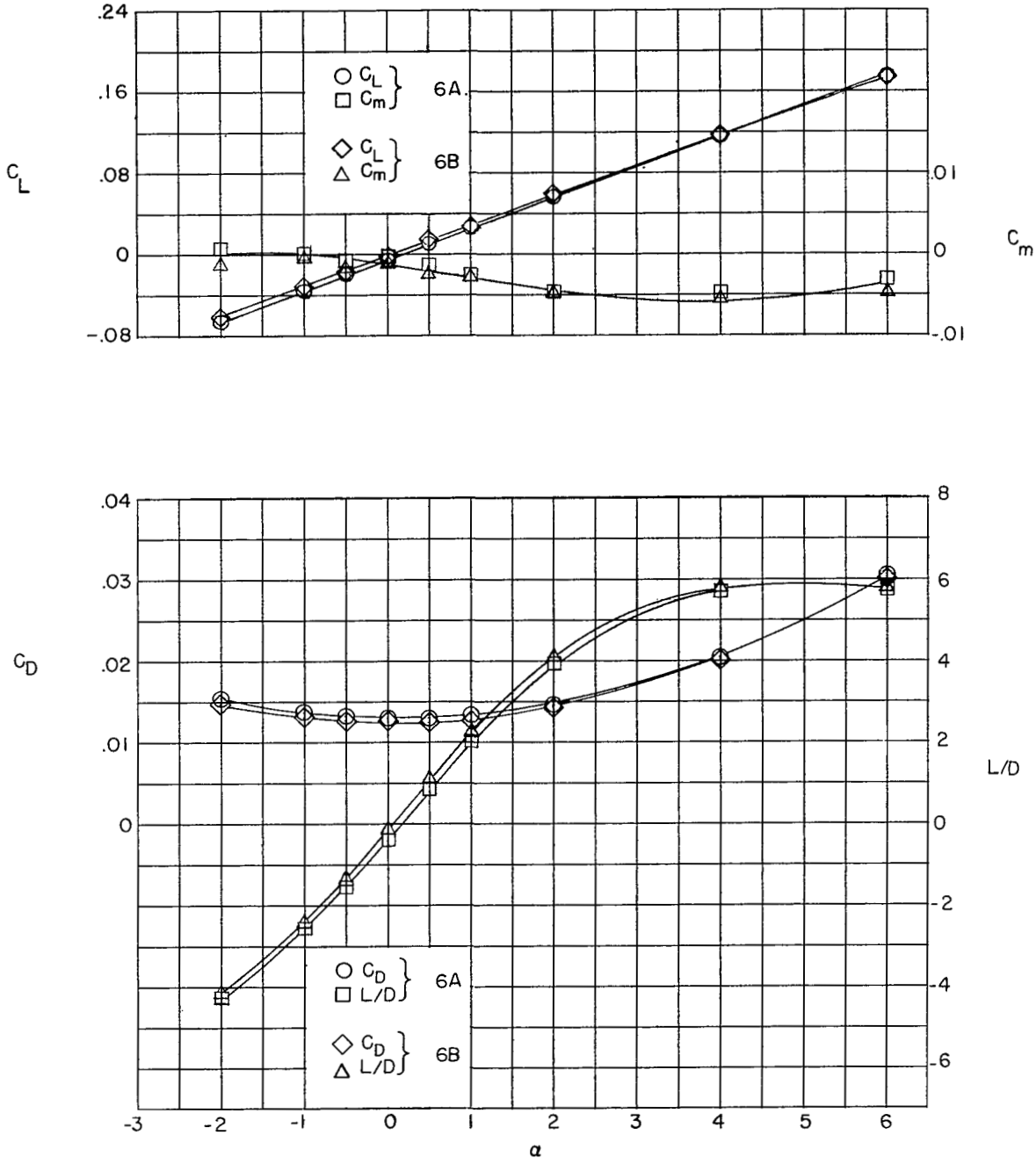

(f) Wings 6A and 6B.

Figure 5.- Continued.

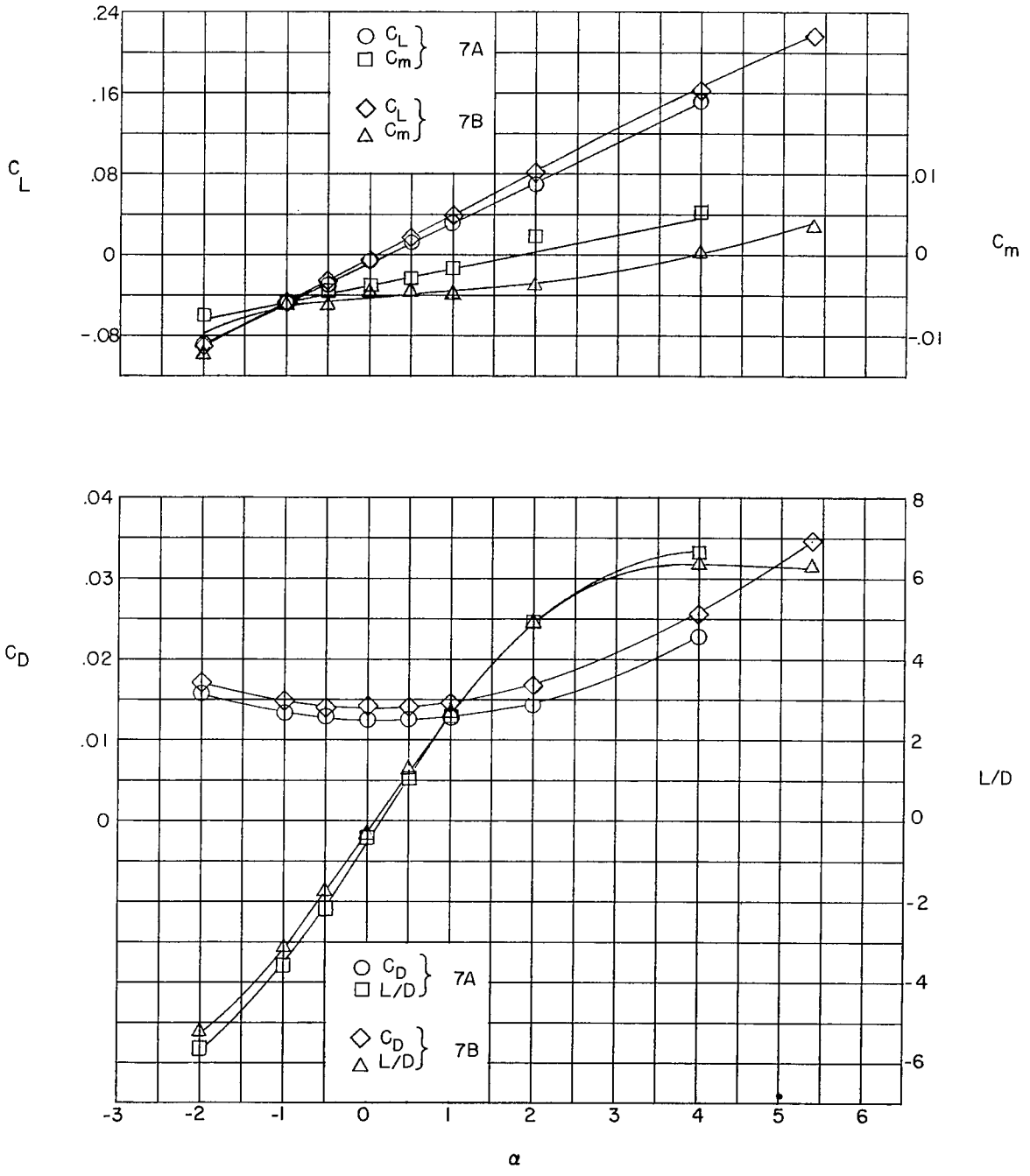

(g) Wings 7A and 7B.

Figure 5.- Concluded.

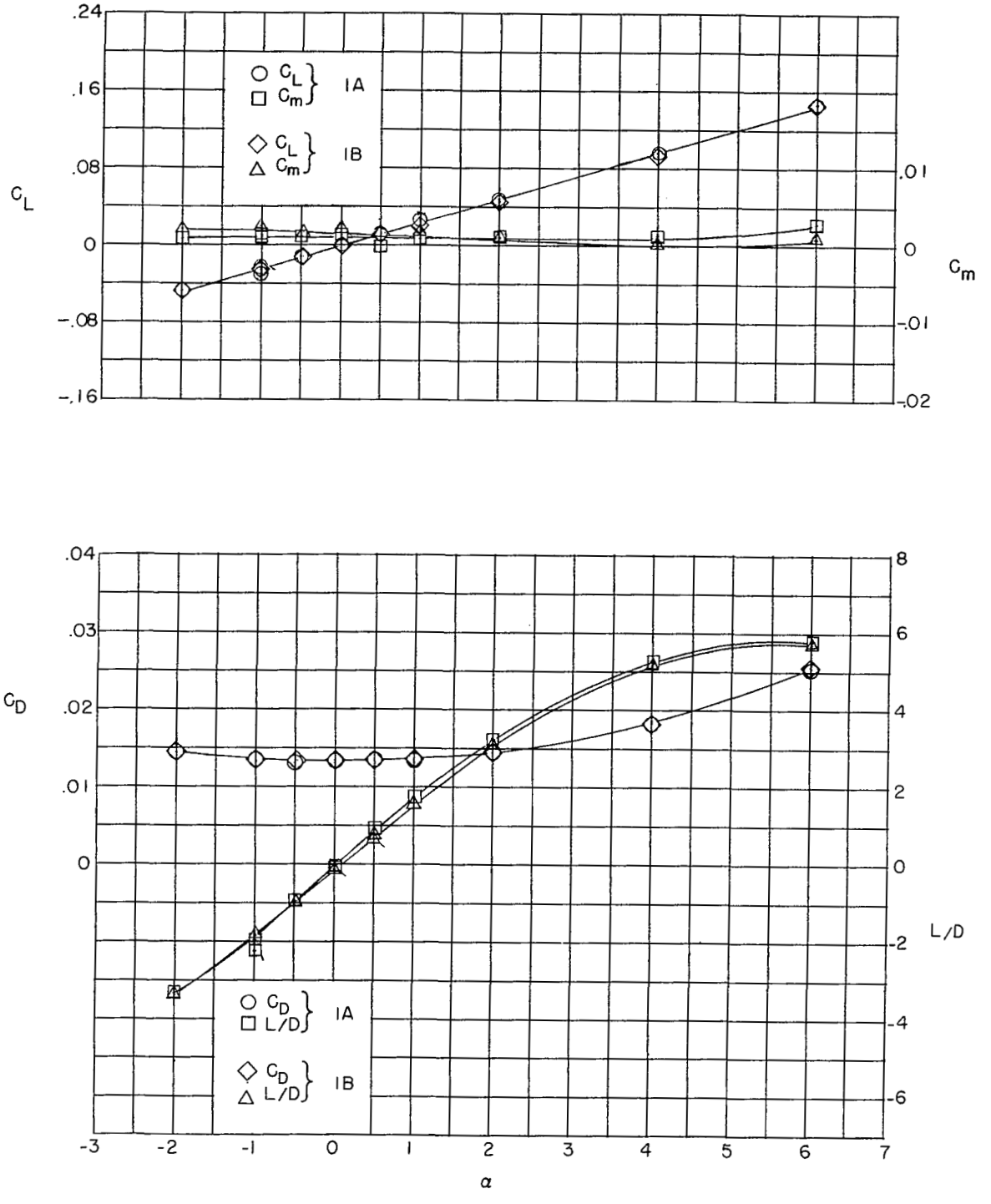

(a) Wings 1A and 1B.

Figure 6.- Aerodynamic characteristics of variable- and constant-thickness-ratio delta wings at M = 2.41. (Flagged symbols represent check points.)

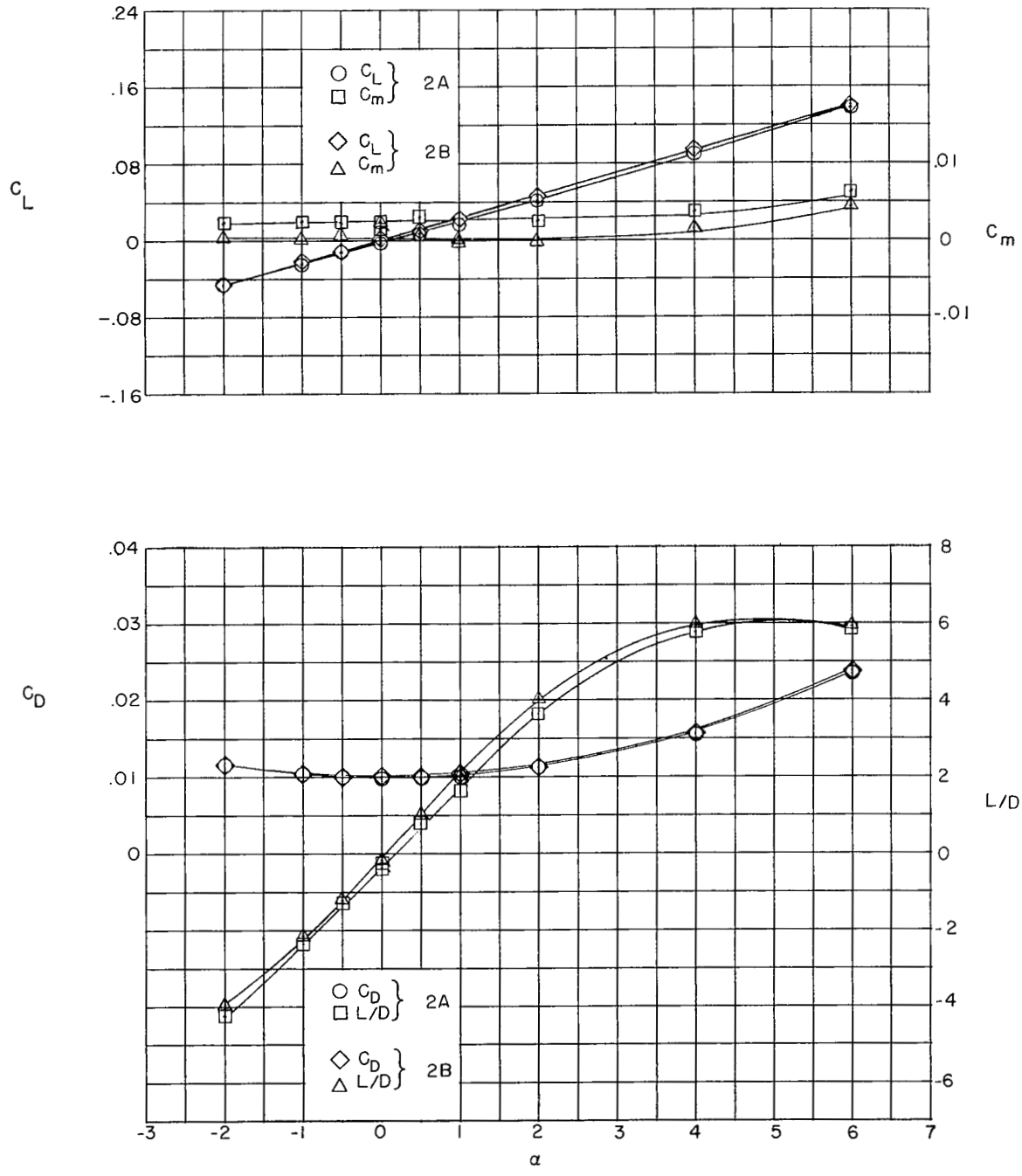

(b) Wings 2A and 2B.

Figure 6.- Continued.

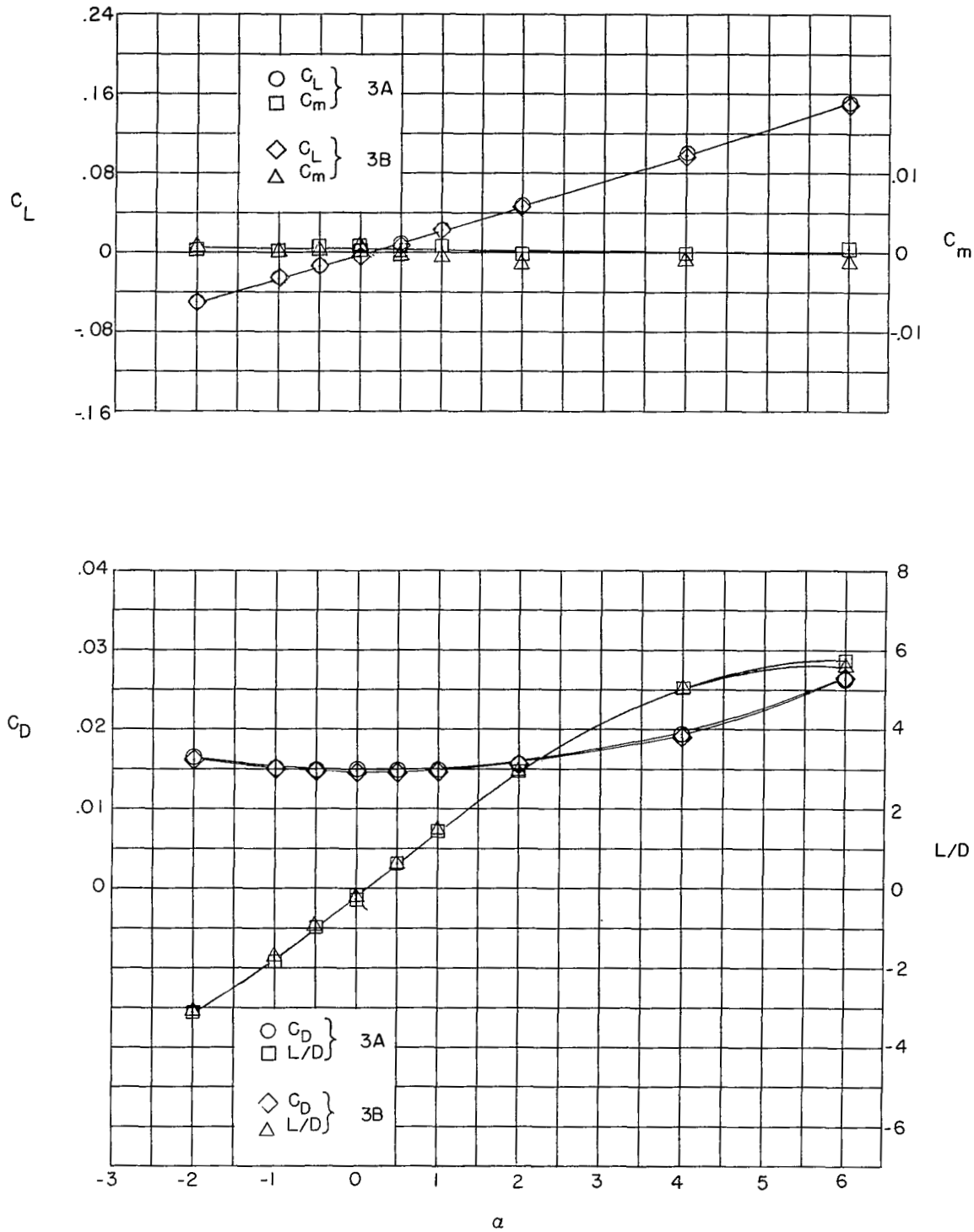

(c) Wings 3A and 3B.

Figure 6.- Continued.

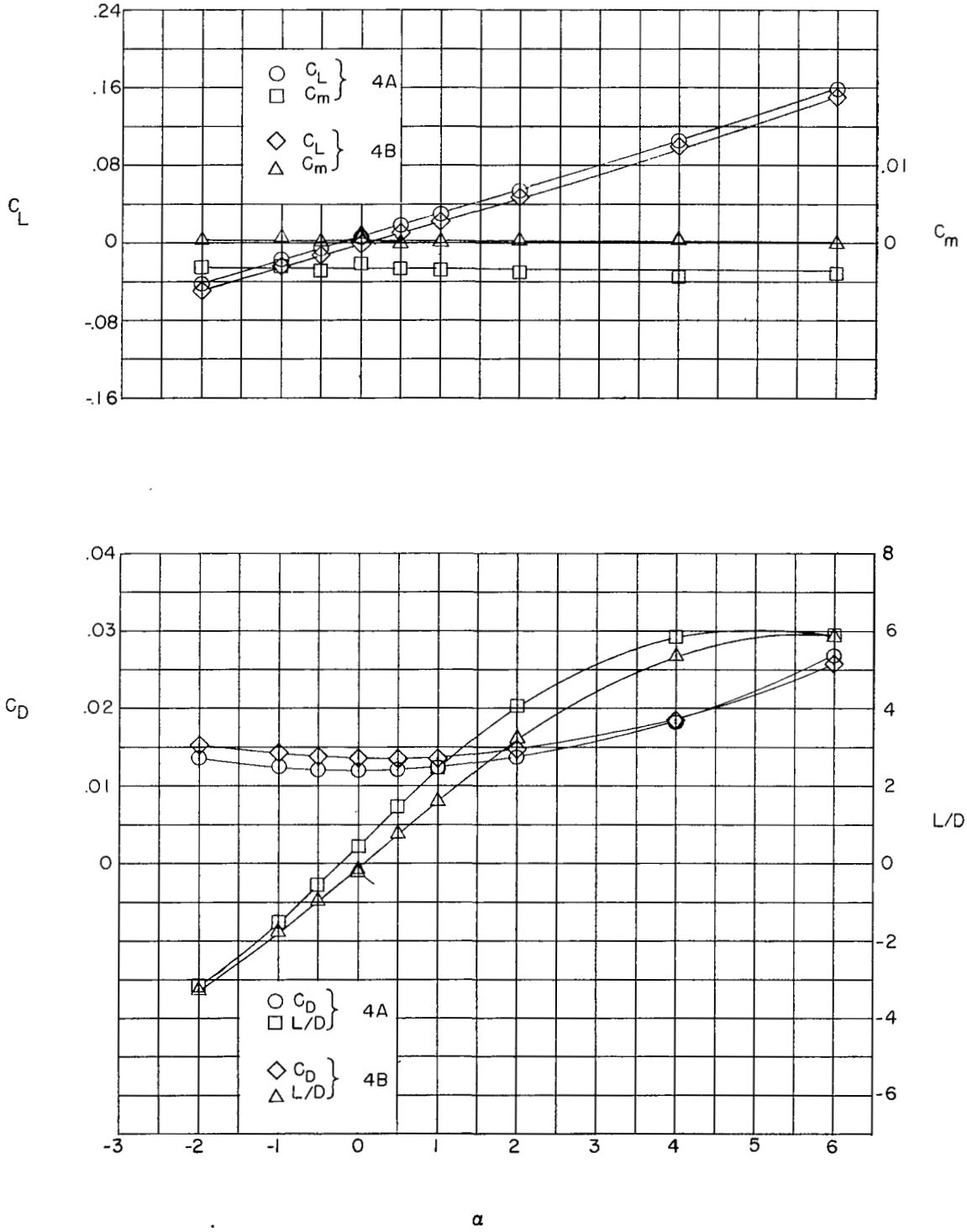

(d) Wings 4A and 4B.

Figure 6.- Continued.

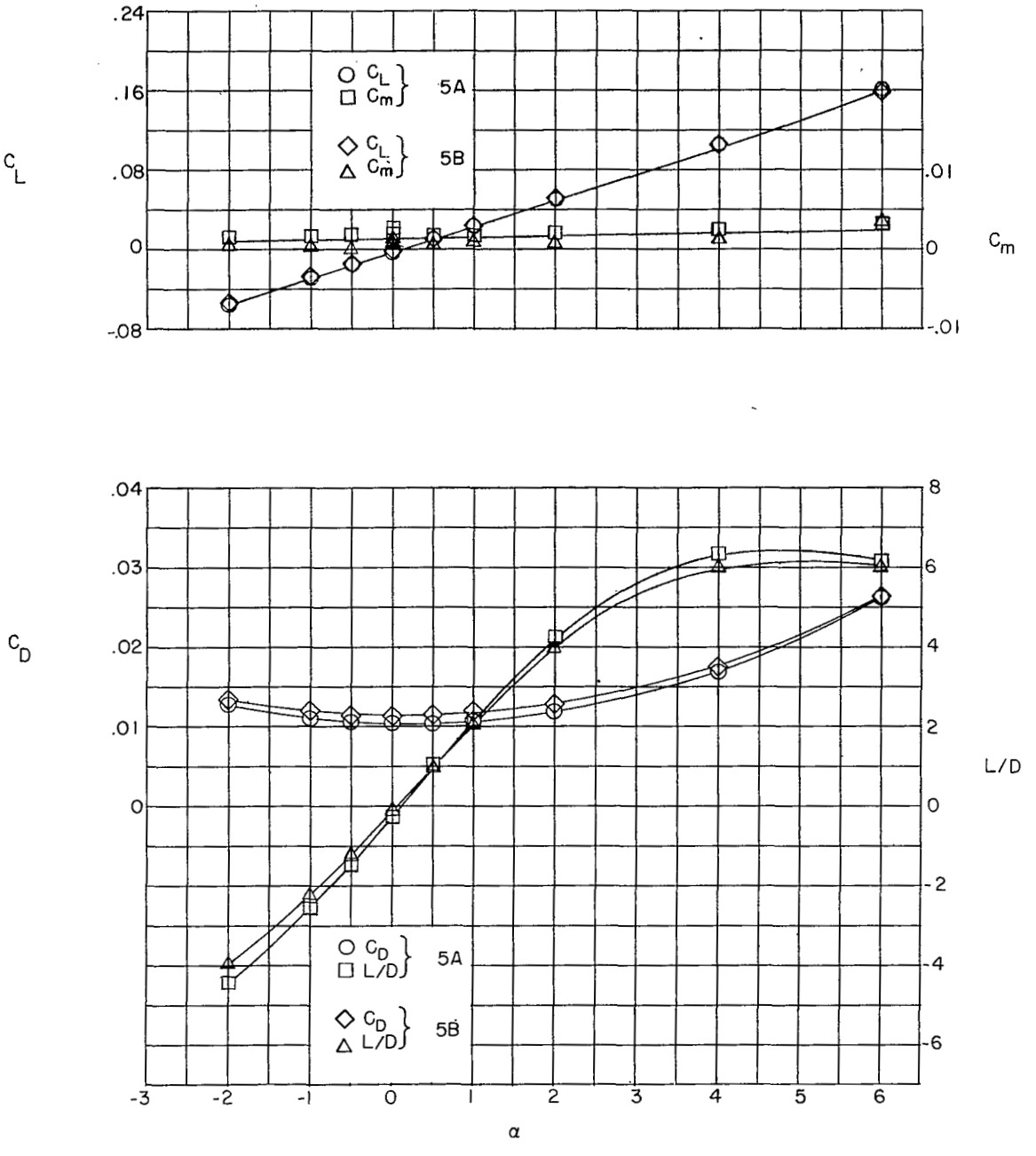

(e) Wings 5A and 5B.

Figure 6.- Continued.

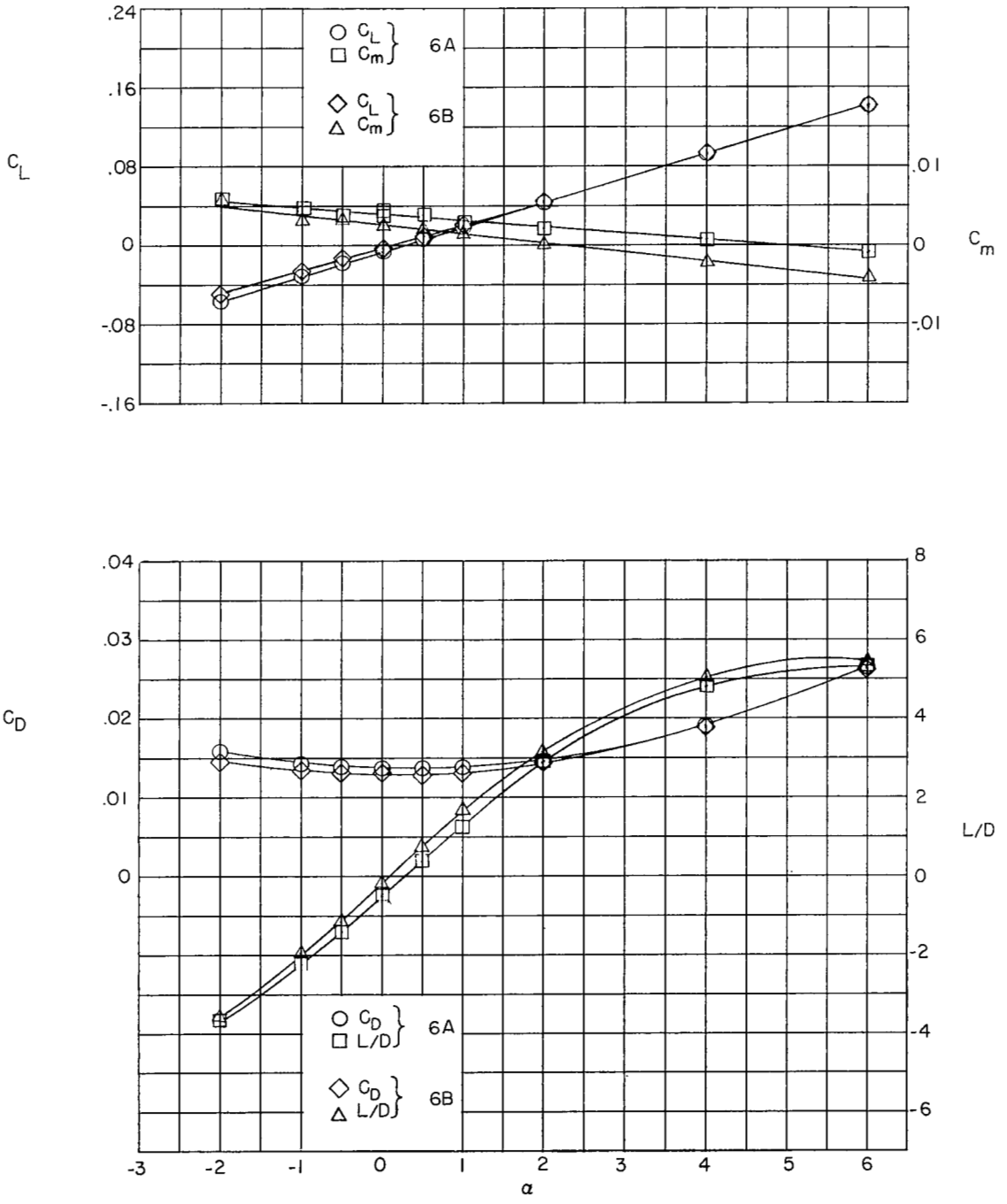

(f) Wings 6A and 6B.

Figure 6.- Continued.

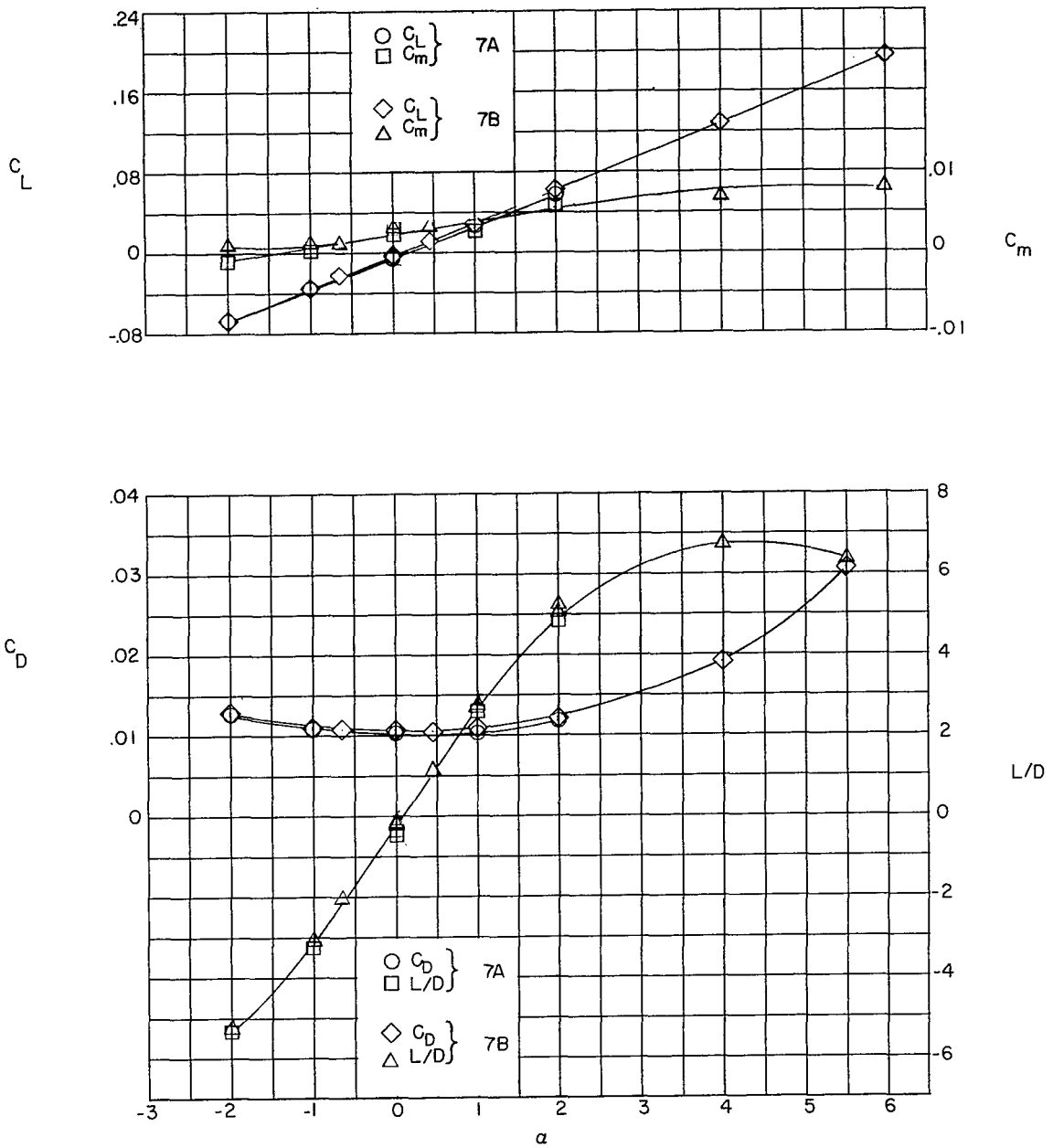

(g) Wings 7A and 7B.

Figure 6.- Concluded.

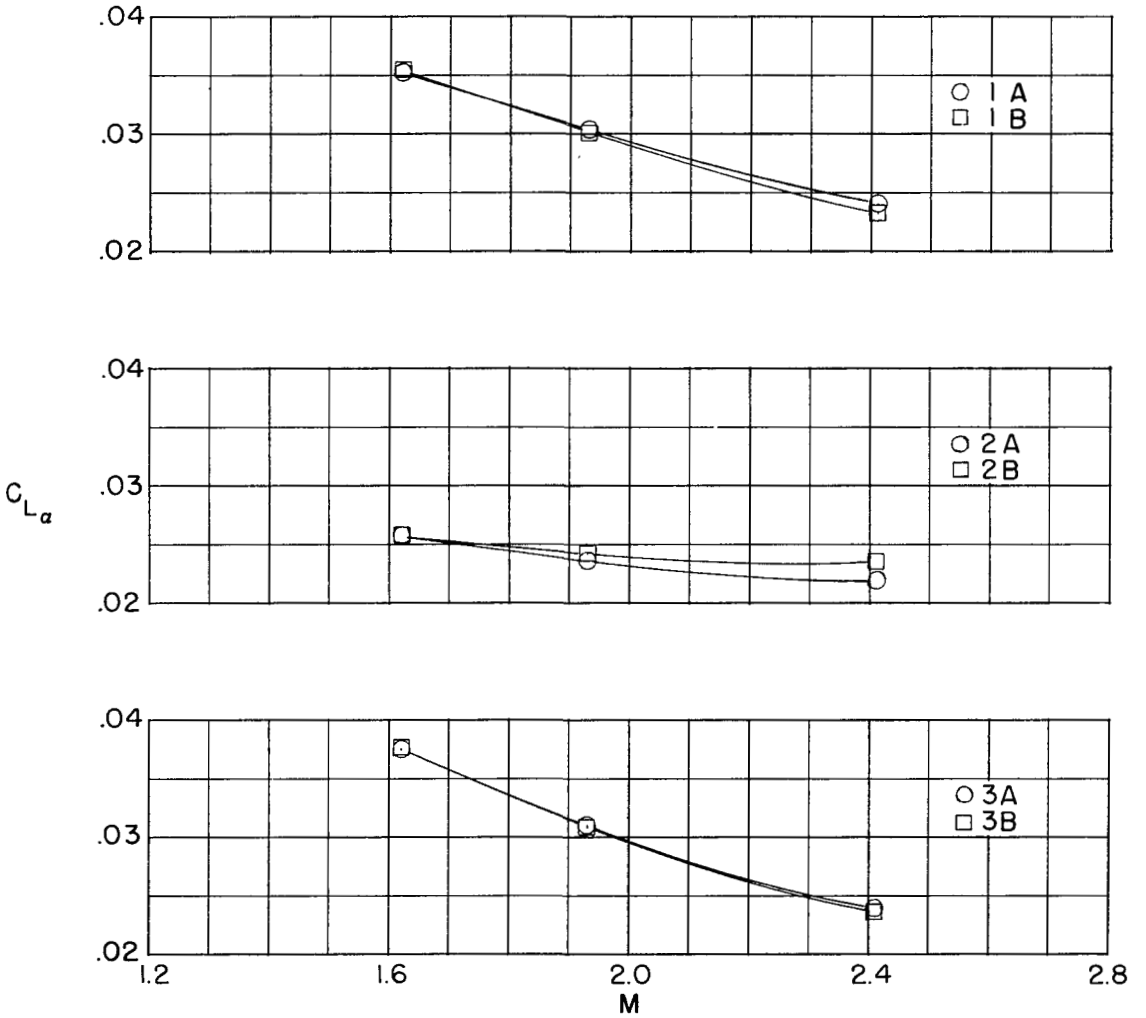

Figure 7.- Lift-curve slopes of variable- and constant-thickness-ratio delta wings.

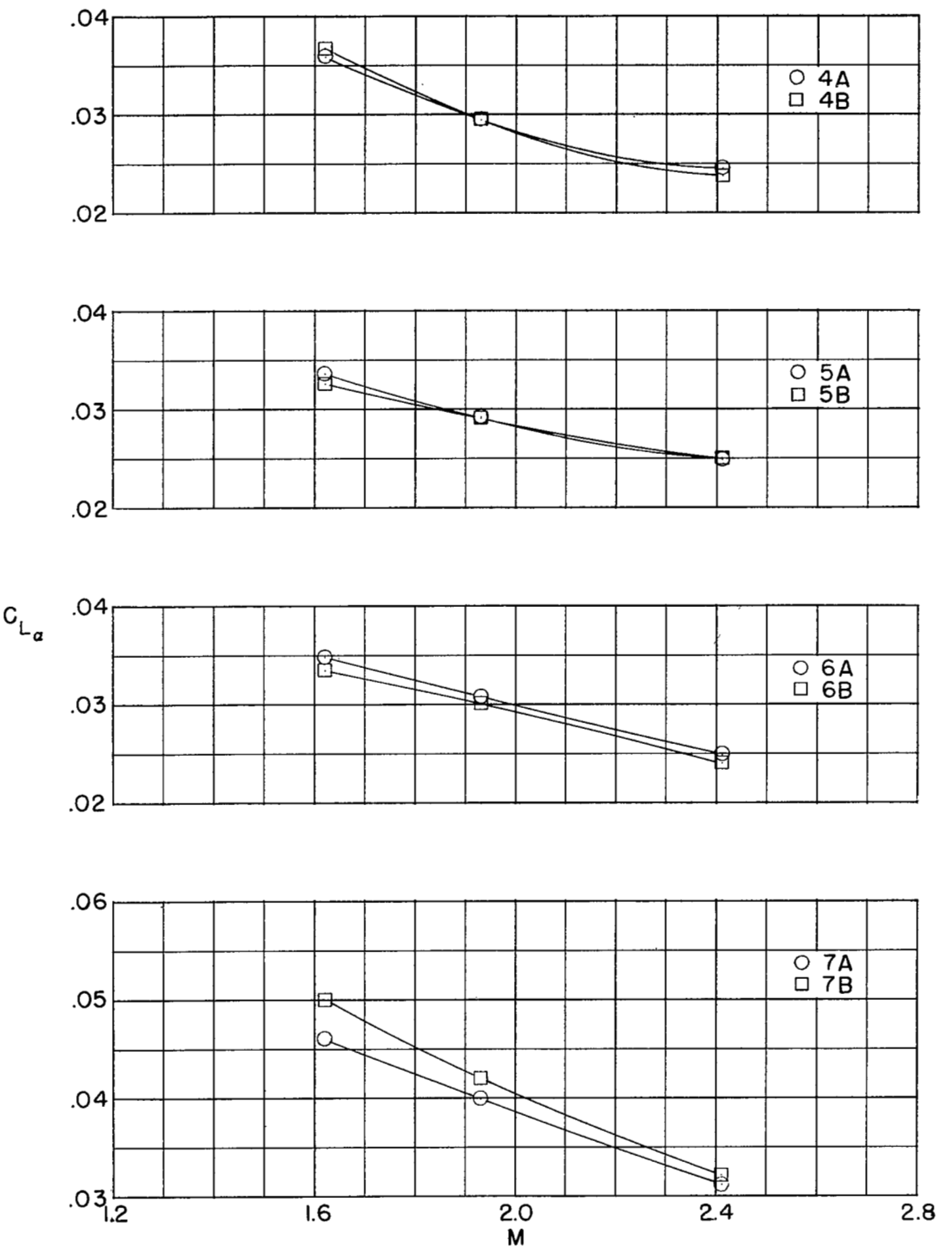

Figure 7.- Concluded.

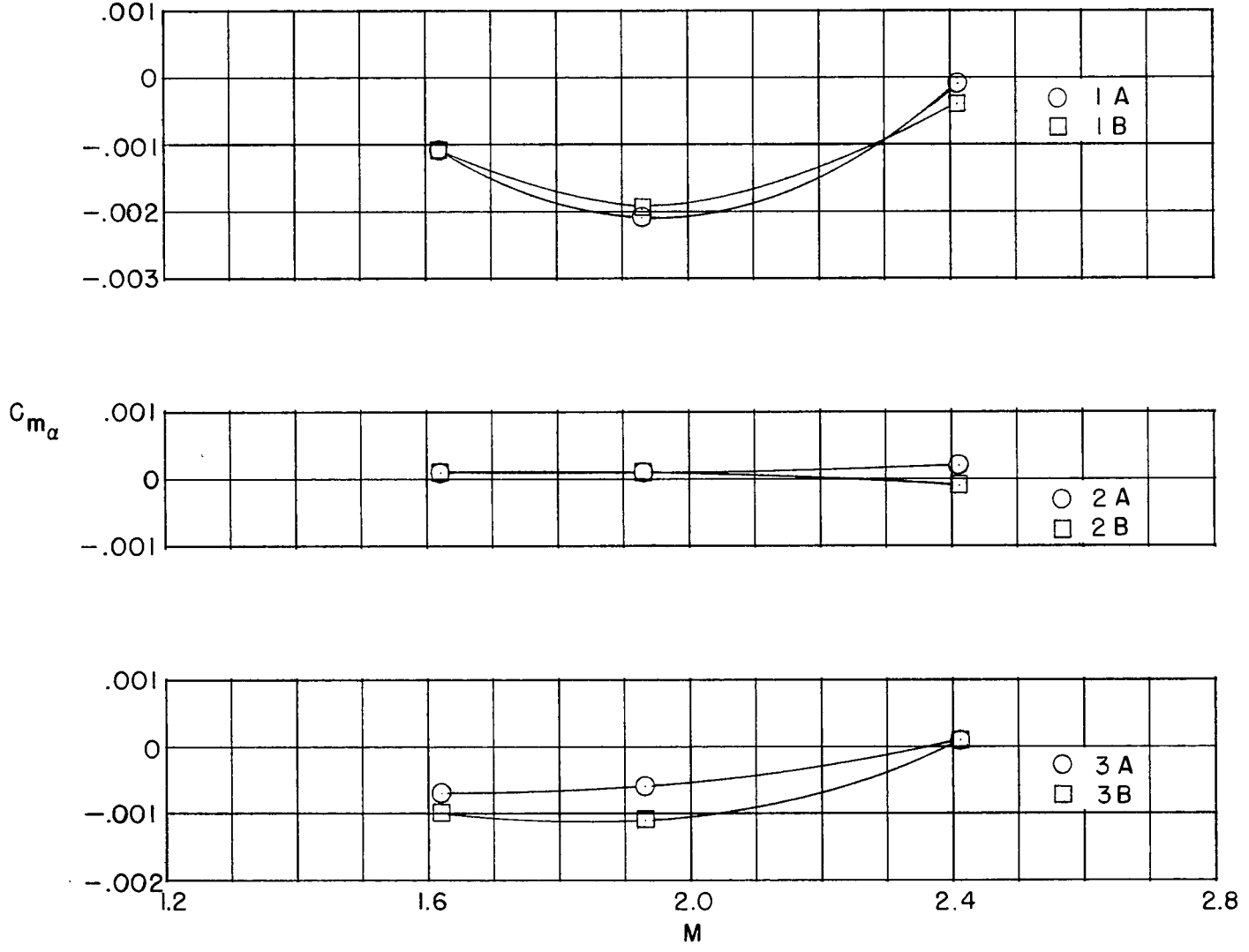

Figure 8.- Moment-curve slopes of variable- and constant-thickness-ratio delta wings.

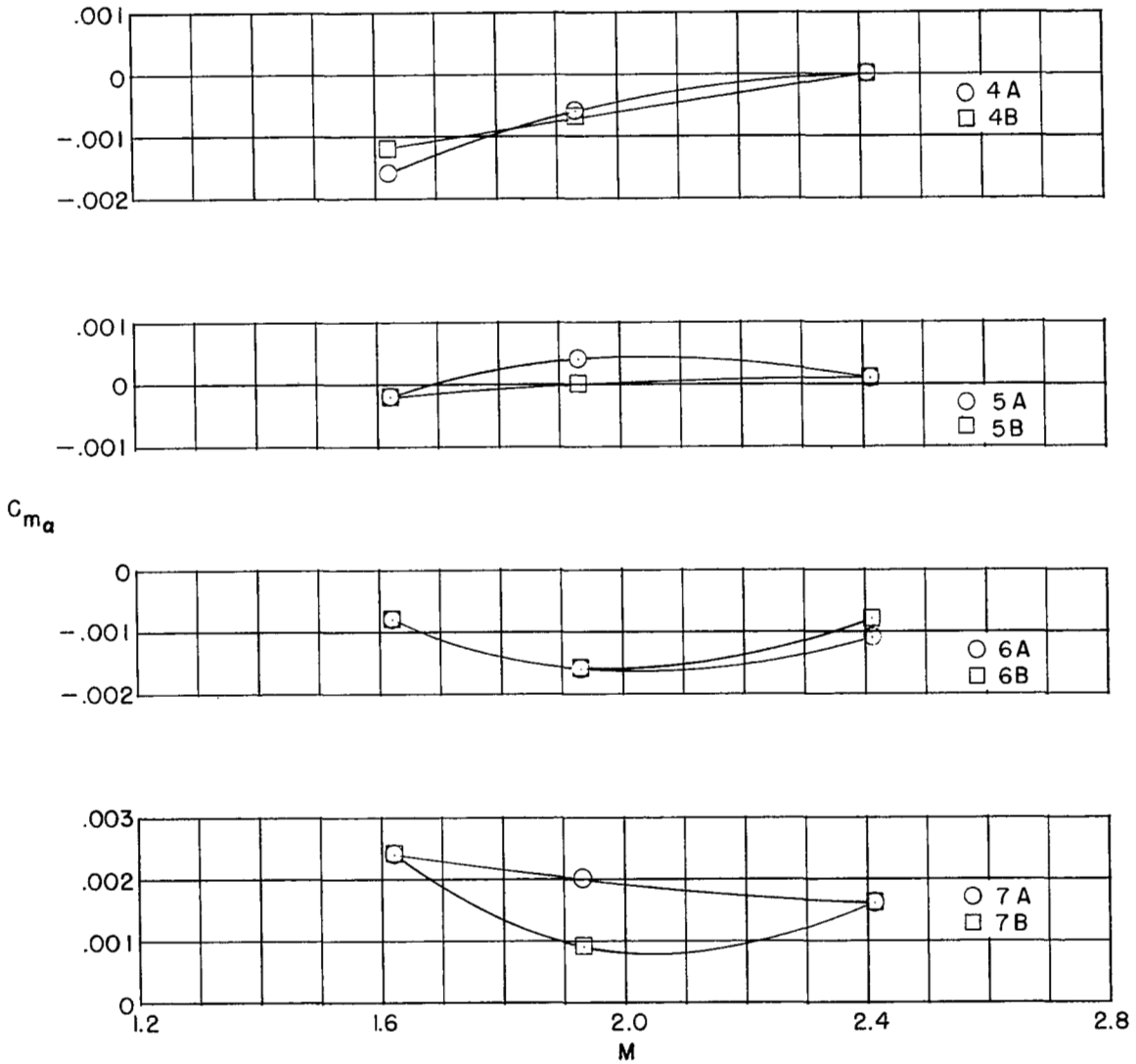

Figure 8.- Concluded.

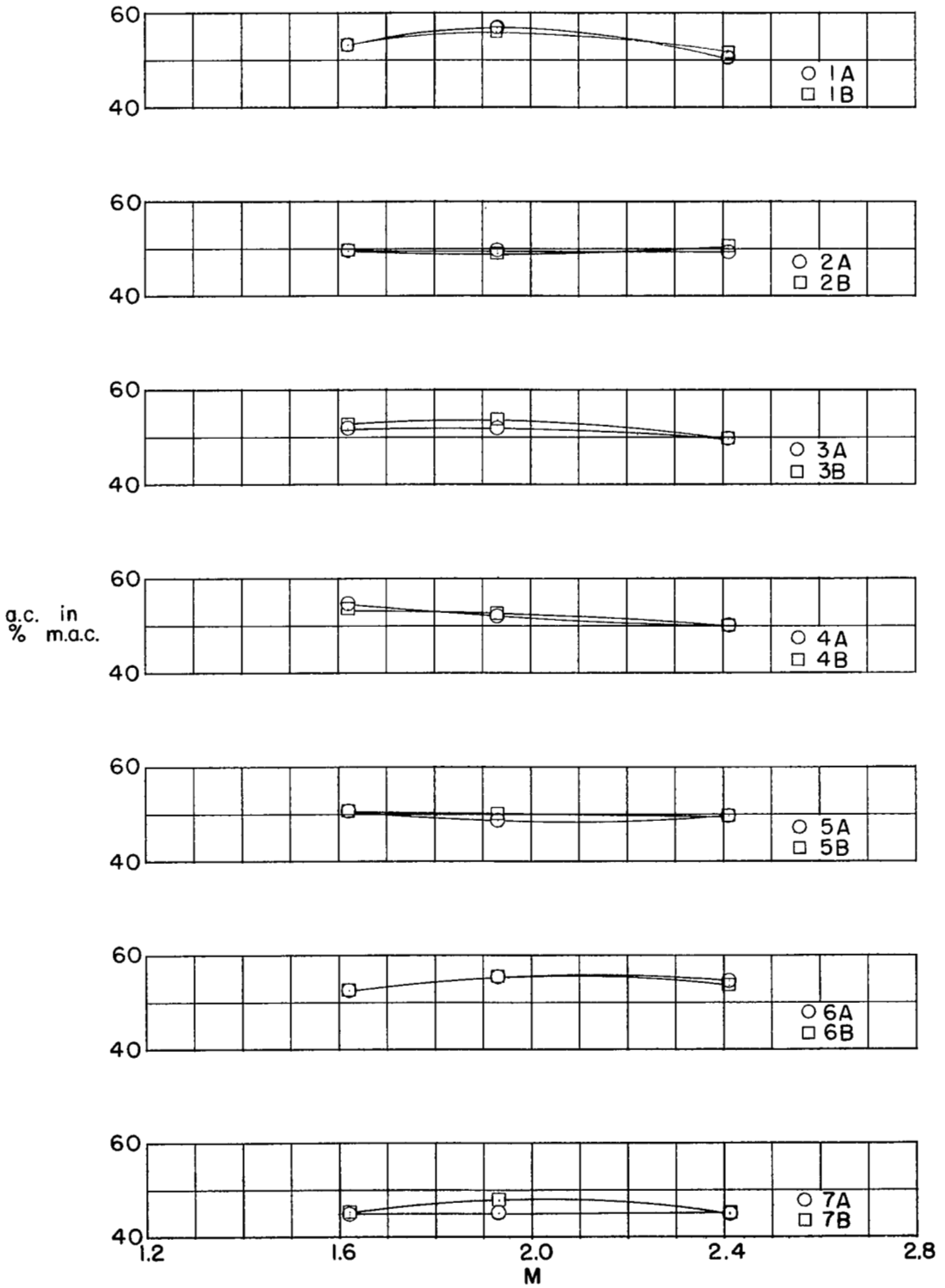

Figure 9.- Location of aerodynamic center of variable- and constant-thickness-ratio delta wings in percent mean aerodynamic chord.

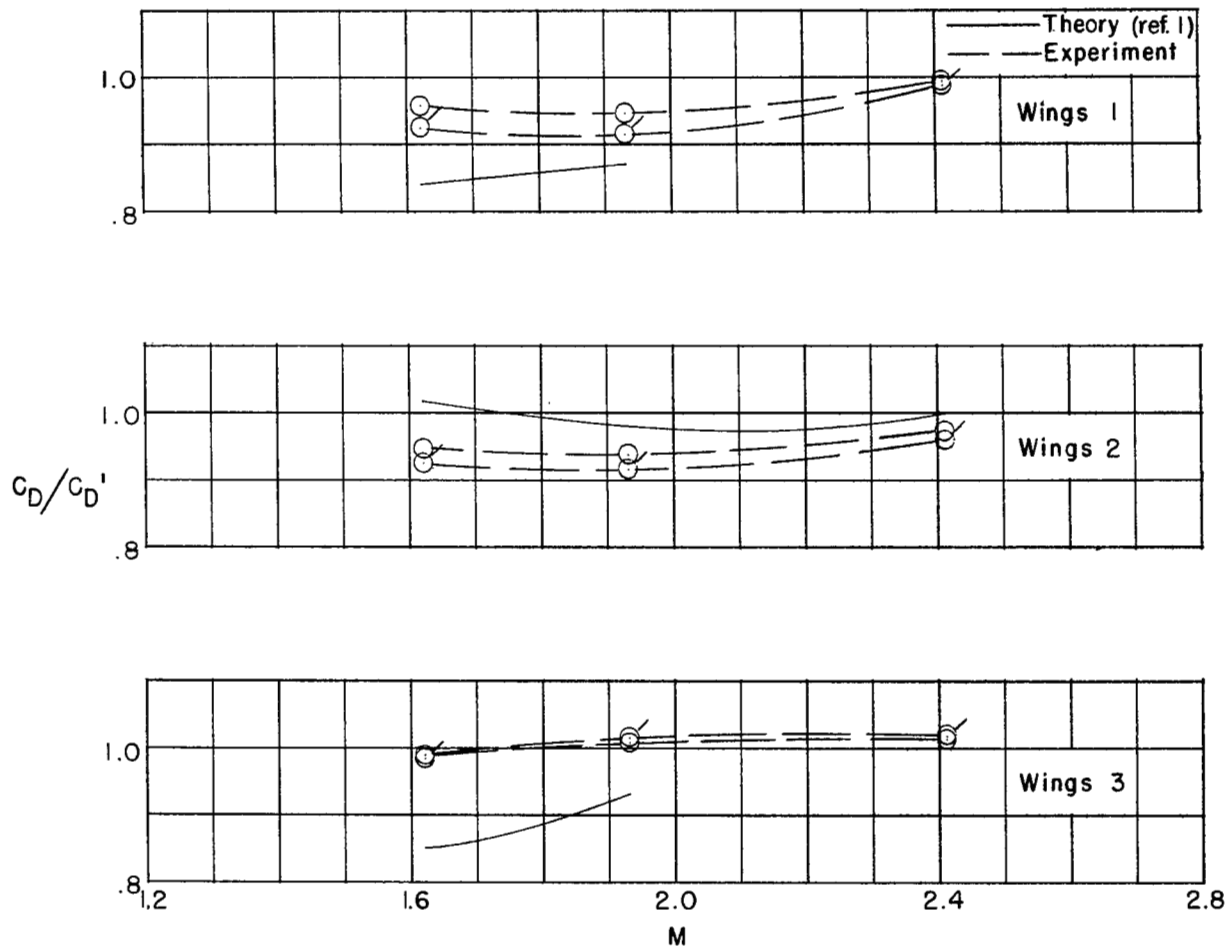

Figure 10.- Ratio of zero-lift drag of variable-thickness-ratio wing to the zero-lift drag of the corresponding constant-thickness-ratio delta wing. Unflagged symbols represent total-drag ratios; flagged symbols represent calculated wave-drag ratios.

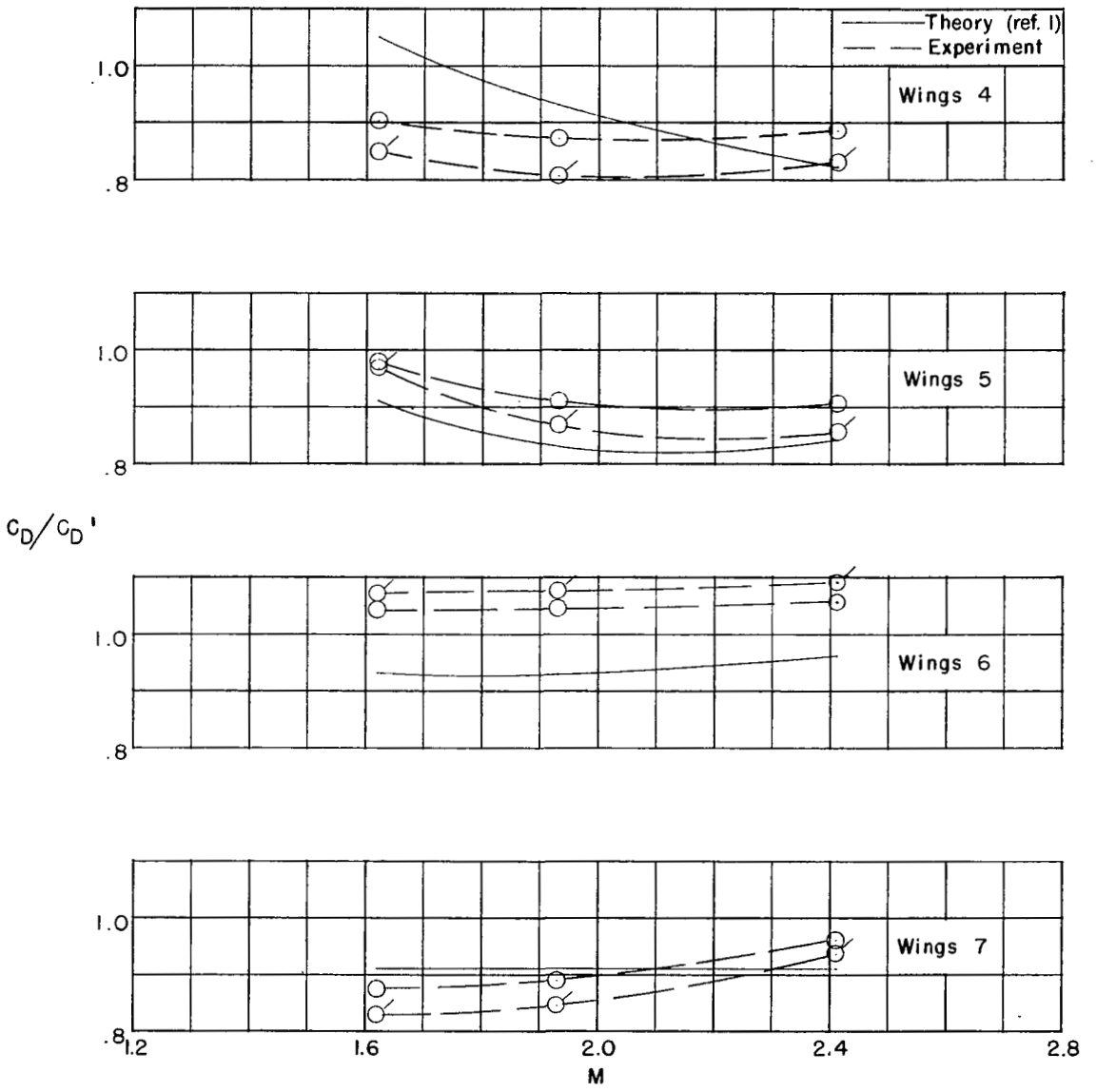

Figure 10.- Concluded.

Figure 11.- Liquid-film pattern for wings 4B and 4A. M = 2.41; R = 3.72 × 10⁶.

L-87925